ORIGINAL ARTICLE

MOLECULAR ECOLOGY WILEY

Stepping up to genome scan allows stock differentiation in the worldwide distributed blue shark *Prionace glauca*

Natacha Nikolic[1,2,3] | **Floriaan Devloo-Delva**[4,5] | **Diane Bailleul**[1] | **Ekaterina Noskova**[6] | **Clément Rougeux**[7] | **Chrystelle Delord**[1] | **Philippe Borsa**[8] | **Cathy Liautard-Haag**[1] | **Mohamad Hassan**[1,9] | **Amandine D. Marie**[3] | **Pierre Feutry**[4] | **Peter Grewe**[4] | **Campbell Davies**[4] | **Jessica Farley**[4] | **Daniel Fernando**[10] | **Sebastian Biton-Porsmoguer**[11] | **François Poisson**[1] | **Denham Parker**[12,13] | **Agostino Leone**[1] | **Jorden Aulich**[4] | **Matt Lansdell**[4] | **Francis Marsac**[1] | **Sophie Arnaud-Haond**[1]

[1]UMR MARBEC, University of Montpellier, IRD, Ifremer, CNRS, Sète, France

[2]INRAE, Ecobiop, AQUA, Saint-Pée-sur-Nivelle, France

[3]ARBRE, Agence de Recherche pour la Biodiversité à la Réunion, Saint-Gilles, France

[4]CSIRO Environment, Hobart, Tasmania, Australia

[5]School of Natural Sciences—Quantitative Marine Science, University of Tasmania, Hobart, Tasmania, Australia

[6]Computer Technologies Laboratory, ITMO University, St Petersburg, Russia

[7]University of Calgary, Calgary, Canada

[8]Institut de recherche pour le développement, UMR ENTROPIE, Montpellier, France

[9]Animal Production Department, Tishreen University, Latakia, Syria

[10]Blue Resources Trust, Colombo, Sri Lanka

[11]French Biodiversity Agency (OFB), Channel and North Sea Delegation, Le Havre, France

[12]Department of Forestry, Fisheries and the Environment, (DFFE), Cape Town, South Africa

[13]Department of Biological Sciences, University of Cape Town, Rondebosch, South Africa

Correspondence
Natacha Nikolic, UMR MARBEC, Univ. Montpellier, IRD, Ifremer, CNRS, Sète, France / INRAE, AQUA, ECOBIOP, Saint-Pée-sur-Nivelle, France.
Emails: natachanikolic@hotmail.com; natacha.nikolic@inrae.fr

Handling Editor: J A H Benzie

Abstract

The blue shark *Prionace glauca* is a top predator with one of the widest geographical distributions of any shark species. It is classified as Critically Endangered in the Mediterranean Sea, and Near Threatened globally. Previous genetic studies did not reject the null hypothesis of a single global population. The blue shark was proposed as a possible archetype of the "grey zone of population differentiation," coined to designate cases where population structure may be too recent or too faint to be detected using a limited set of markers. Here, blue shark samples collected throughout its global range were sequenced using a specific RAD method (DArTseq), which recovered 37,655 genome-wide single nucleotide polymorphisms (SNPs). Two main groups emerged, with Mediterranean Sea and northern Atlantic samples (Northern

Natacha Nikolic and Floriaan Devloo-Delva contributed equally.

population) differentiated significantly from the Indo-west Pacific samples (Southern population). Significant pairwise F_{ST} values indicated further genetic differentiation within the Atlantic Ocean, and between the Atlantic Ocean and the Mediterranean Sea. Reconstruction of recent demographic history suggested divergence between Northern and Southern populations occurred about 500 generations ago and revealed a drastic reduction in effective population size from a large ancestral population. Our results illustrate the power of genome scans to detect population structure and reconstruct demographic history in highly migratory marine species. Given that the management plans of the blue shark (targeted or bycatch) fisheries currently assume panmictic regional stocks, we strongly recommend that the results presented here be considered in future stock assessments and conservation strategies.

1 | INTRODUCTION

The blue shark *Prionace glauca* is distributed worldwide and considered the most abundant pelagic shark (Compagno, 1984; Nakano & Seki, 2003). Occurring in all oceans, its habitat extends from the surface to >1100 m depth except in polar regions (i.e., from 60° N to 50° S) of the world oceans (Queiroz et al., 2012). Like other top predators (Estes et al., 2011; Hughes et al., 2013), the blue shark contributes to the top-down regulation of marine communities, and thus to the stability and persistence of the pelagic marine ecosystems across its vast distribution (e.g., Hernández-Aguilar et al., 2015).

The blue shark is the most frequently fished shark species worldwide (Baum & Blanchard, 2010; Biton-Porsmoguer, 2018; Campana et al., 2006) along with shortfin mako and pelagic thresher sharks (Megalofonou, Yannopoulos, et al., 2005). Although occasionally targeted for its meat on the western coast of Baja California Sur (Galván-Magaña et al., 2019) and by recreational fisheries (Campana et al., 2006; Mejuto & Garcia-Cortés, 2005; Panayiotou et al., 2020), the blue shark is mostly a bycatch of tuna and swordfish longline fisheries (Biton-Porsmoguer, 2017; Biton-Porsmoguer & Lloret, 2018; Carvalho et al., 2015; Coelho et al., 2017). The bycatch mortality rate on pelagic longline fishing operations can be high, up to 35%, with an additional post-release mortality at 19% (Campana et al., 2009). The blue shark is also the main species involved in the shark fin trade (Clarke et al., 2006), in which the fins are retained and the body is most often discarded because of its lower commercial value. Despite not being particularly targeted for its meat, with an estimate of 10–20 million individuals caught annually (Megalofonou et al. 2005b; Stevens, 2009), the blue shark has been evaluated as Near Threatened worldwide (Rigby et al., 2019; Stevens, 2009) and Critically Endangered in the Mediterranean Sea (Sims et al., 2016).

Evidence of a 90% decline in blue shark abundance has been reported in the Mediterranean Sea (Ferretti et al., 2008). Population declines have also been reported in both the Atlantic

(Aires-da-Silva et al., 2008, 2009; Baum & Blanchard, 2010; Simpfendorfer et al., 2002) and the Pacific (Clarke et al., 2013) oceans, but some other studies in the same areas indicate that the catch per unit of effort might be stable, or even slightly increasing (ISC, International Scientific Committee for Tuna and Tuna-like Species in the north Pacific Ocean, 2018; Matsunaga & Nakano, 1999; Nakano & Clarke, 2005; Nakano & Stevens, 2008). These inconsistencies point to a poor understanding of the biology and ecology of the blue shark and to the difficulties in estimating its abundance. Intergovernmental bodies have acknowledged the need to fill important ecological and biological data gaps to improve stock assessments in the blue shark, which in turn can be used to provide advice on fisheries management (IOTC, 2017; ISC, 2018). The International Commission for the Conservation of Atlantic Tunas (ICCAT) acknowledged the steady increase of blue shark catches in recent years and the large level of uncertainty in the data inputs and model assumptions about the stock and the fishery. In 2019, the ICCAT adopted recommendations to further limit blue shark catches and encouraged further research to provide essential knowledge needed for its long-term management, including life-history parameters and migrations (ICCAT, 2019).

Given the blue shark's highly migratory behaviour and its wide distribution (Stevens, 1990), fisheries managers rely on the assumption that stocks in the northern and southern Atlantic (ICCAT, 2015), in the northern and southern Pacific (ISC, 2018), and in the Indian (IOTC, 2017) oceans are regionally homogeneous. Electronic tags have confirmed that blue sharks swim over large distances, even crossing from one ocean to another (da Silva et al., 2010; Kohler et al., 2002; Maxwell et al., 2019; Queiroz et al., 2012; Vandeperre et al., 2014). However, nonoverlapping reproductive cycles have been reported in the Northern and Southern Hemispheres (Nakano & Seki, 2003; Nakano & Stevens, 2008) and transequatorial migration is assumed to be limited (Kohler and Kohler & Turner, 2008).

Based on mitochondrial DNA or/and microsatellite markers, no consistent pattern of genetic differentiation has been detected, even between the Northern and Southern Hemispheres (Bitencourt et al., 2019; King et al., 2015; Li et al., 2017; Taguchi et al., 2015; Verissimo et al., 2017). Only weak differentiation of the Mediterranean Sea population (Bailleul et al., 2018; Leone et al., 2017), and among the southeastern Pacific and Western Australian sampling locations (Taguchi et al., 2015) was detected. Traditional genetic approaches only detect extreme restriction to gene flow, far below the threshold of demographic independence (Waples, 1998; Waples & Gaggiotti, 2006), and integrate migration over an often large number of generations that is proportional to effective population size (Hedgecock et al., 2007). In marine species, effective population size can be extremely large, a situation that probably applies to the blue shark considering its wide distribution and relatively high abundance. In fact, the blue shark has been used as a case species to illustrate the concept of "population grey zone" (Bailleul et al., 2018), which refers to the often-inconclusive results of population genetic differentiation studies. The "population grey zone" effect describes the potentially very long time-lag (hundreds to thousands of generations) between the demographic split of a population into two independent demographic entities and its translation into a genetic signal strong enough to be detected by a handful of molecular markers (Bailleul et al., 2018). Genome scan methods such as restriction site-associated DNA sequencing (RADseq; Davey & Blaxter, 2010) or Diversity Arrays Technology sequencing (DArTseq; DArT Pty Ltd: Georges et al., 2018) provide a much denser array of markers, typically thousands of single nucleotide polymorphisms (SNPs) along the genome, increasing the power to detect subtle levels of genetic differentiation (Foster et al., 2021). The recent use of genome scans to detect genetic structure in large pelagic species including yellowfin tuna (Grewe et al., 2015; Mullins & Shaw, 2018; Pecoraro et al., 2018), striped marlin (Mamoozadeh et al., 2020), spotted dolphin (Leslie & Morin, 2016) and Atlantic mackerel (Rodríguez-Ezpeleta et al., 2016) provided a much higher resolution than traditional genetic markers and revealed genetic structure where no or only weak, sometimes incongruent, patterns of differentiation had initially been detected.

Here, we used the DArTseq sequencing approach on blue shark samples collected from the Atlantic, Pacific and Indian Oceans, as well as from the Western Mediterranean Sea, to test the null hypothesis of large-scale panmixia. Preliminary results on basic population differentiation have been presented previously (Nikolic et al. 2020a). In this paper we provide a more comprehensive analysis of the blue shark population genetic structure as well as infer its demographic history for the first time. We take advantage of the power offered by genome scan analysis to delineate potential management units, and to investigate the demographic history up to the most recent decades, which were marked by increasing fishing pressure on blue shark populations worldwide (IOTC, 2017; Nakano & Seki, 2003; Porcher & Darvell, 2022).

2 | MATERIALS AND METHODS

2.1 | Sampling

A total of 376 individual blue sharks were sampled by scientists (90%) and fishermen (10%) between 2009 and 2018, and 364 individuals were successfully genotyped (29 individuals sampled in 2009, eight in 2010, four in 2011, 24 in 2012, 56 in 2013, 39 in 2014, 81 in 2015, three in 2017 and 120 in 2018) across several geographical regions throughout the species range (Figure 1). All were caught by longline as bycatch, except the samples from the eastern Indian Ocean where individuals were caught by purse seine. Only dead individuals were sampled. Individual length (cm) and phenotypic sex (based on the presence or absence of claspers), geographical location (latitude and longitude) and details on operating vessel were recorded—except for 93 individuals missing length data and 149 individuals whose sex was not identified. Whenever applicable, curved fork length, precaudal length and interdorsal (space on the dorsal surface between the first and second dorsal fins) were converted to fork length (FL) based on the equations of Cramer et al. (1997). A small piece of fin, skin or muscle was preserved in 96% ethanol at all sampling locations except the eastern Indian Ocean samples, tissues of which were dried in silica gel, and Reunion Island samples, tissues of which were preserved in RNAlater solution (Qiagen).

2.2 | DArT library preparation and sequencing

Genomic DNA was extracted from 15 mg of muscle tissue subsampled from individual biopsies on an Eppendorf EP Motion 5057 liquid robotic handler using a modification of the QIAamp 96 DNA QIAcube HT Kit (Qiagen). This extraction included a lysis step in the presence of proteinase K followed by bind-wash-elute Qiagen processing. Low-quality or degraded samples were extracted using the modified CTAB method of Grewe et al. (1993).

Genomic DNA was processed for the construction of a reduced representation library, sequenced and genotyped by using the DArTseq technique. DNA sample libraries were created through digestion and ligation reactions using two methylation-sensitive restriction enzymes, *Pst*I and *Sph*I. The *Pst*I site was compatible with a forward adapter that included a flow cell (Illumina) attachment sequence and a sequencing primer sequence incorporating a staggered, barcode region of varying length. The *Sph*I digestion generated a compatible overhang sequence that was ligated to a reverse adapter containing a flow cell attachment region and a reverse-priming sequence. Only mixed *Pst*I–*Sph*I restriction fragments were amplified by PCR (polymerase chain reaction). PCR conditions consisted of an initial denaturation at 94°C for 1 min followed by 30 cycles of 94°C for 20 s, 58°C for 30 s and 72°C for 45 s, with a final extension step at 72°C for 7 min. After PCR, equimolar amounts of amplification products from each sample of the
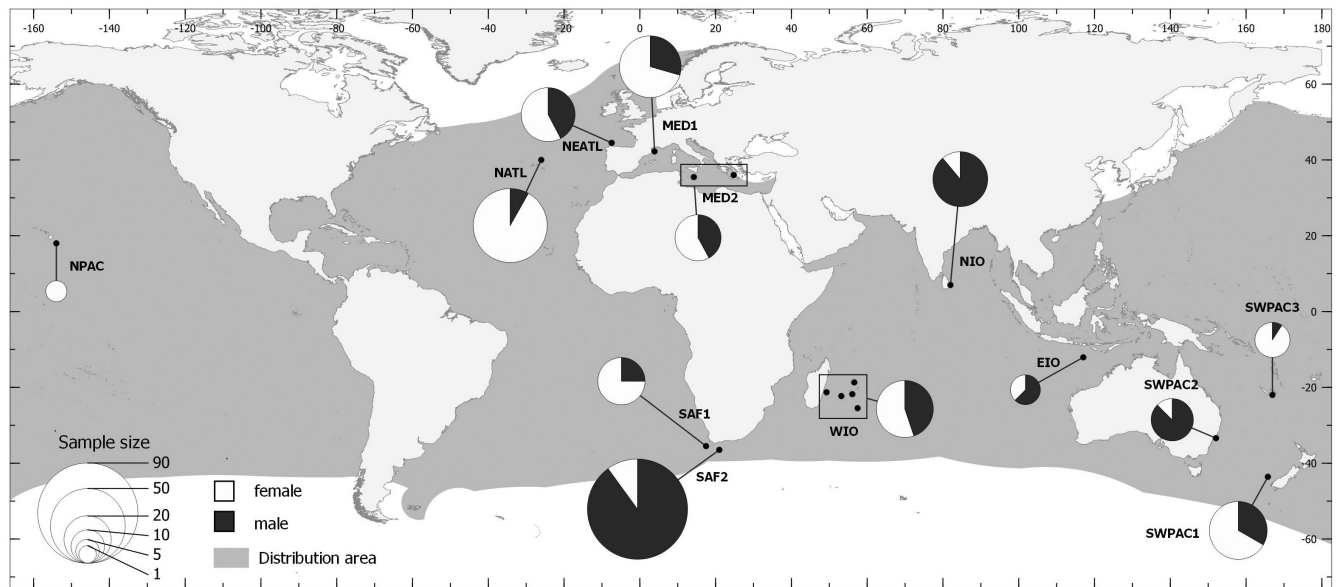
FIGURE 1 Location of blue shark, *Prionace glauca*, sample sites across several geographical regions (364 genotyped individuals). Circle area is proportional to the number of individuals. Black and white colours indicate sex as identified from genetic markers and biological identification. Geographical regions are Mediterranean (MED: MED1, *n* = 34 individuals; and MED2, *n* = 20), northern Atlantic (NATL, *n* = 49), northeastern Atlantic (NEATL, *n* = 26), South Africa (SAF: SAF1, *n* = 21; and SAF2 *n* = 89), eastern Indian Ocean (EIO, *n* = 8), northern Indian Ocean (NIO, *n* = 27), western Indian Ocean (WIO, *n* = 29), southwestern Pacific (SWPAC: SWPAC1, *n* = 30; SWPAC2, *n* = 16; and SWPAC3, *n* = 11) and northeastern Pacific (NPAC, *n* = 4). Shaded: Species distribution area, from Compagno (1984) and the IUCN red list (https://www.iucnredlist.org/species/39381/2915850; accessed June 22, 2022).

96-well microtitre plate were bulked and subjected to cBot bridge PCR (Illumina), followed by sequencing on an Illumina Hiseq2000 automated sequencing system. The sequencing (single-end) was run for 77 cycles. The DNA fragments selected by this process were ~75 bp long. Further details on this sequencing method can be found in Sansaloni et al. (2011), Kilian et al. (2012) and Georges et al. (2018).

2.2.1 | SNP genotyping process

For initial assessment of read quality and sequence representation, raw reads (raw data, Figure 2) were processed using the Illumina Consensus Assessment of Sequence And VAriation (CASAVA) version 1.8.2 software. Genotypes were generated from sequencing runs completed at DArT using a proprietary DArTseq analytical pipeline (DArT-Soft14 version). The DArT toolbox was then used to filter away poor-quality sequences, apply more stringent selection criteria to the barcode region and generate the final genotypes (Kilian et al., 2012), here called one-row data (Figure 2). Details of the bioinformatic steps leading to SNP genotyping can be found in Georges et al. (2018).

2.2.2 | SNP filtering

Multiple steps were performed in the data analysis, each using the appropriate software. Details of the scripts for SNP filtering and

data analyses are presented in an R Markdown report (https://cloud.r-project.org/package=rmarkdown; Allaire et al., 2020) as Appendix S1. Here, we provide an overview of the process followed for SNP filtering, on individual samples grouped per geographical region (Filtration 1) or per sampling site (Filtration 2).

First, metadata with all information on the individuals including sampling location, sex and length, and one-row data with both SNP and reference alleles where a zero (0) score denotes a homozygote, one (1) a homozygote, and two (2) a heterozygote, were merged to build the data set called DATA 1 (Figure 2). Then, SNPs from DATA 1 were filtered for low reproducibility based on technical replicate libraries, monomorphism across all individuals, low minor allele count, low coverage per locus, high missing data per SNP, short-linkage disequilibrium by keeping one SNP per locus, and SNPs out of Hardy–Weinberg equilibrium (HWE) using the RADIATOR package version 1.2.0 (Gosselin, 2018; Gosselin et al., 2020) in R version 4.1.0 (R Development Core Team 2020) (see details in Appendix S1). Individuals were filtered based on high missing data, high heterozygosity and duplicate individuals. At this stage, the data set was called DATA 2 (Figure 2).

Sex-linked marker identification

The unfiltered data (DATA 1) were tested for the presence of sex-linked markers using the *sexy_markers* function in the RADIATOR package (Gosselin et al., 2020). To eliminate erroneous detections, the DATA 1 data set was filtered for high individual missing data and heterozygosity, as well as monomorphic markers and short-distance linkage of SNPs. Subsequently, we identified markers on the Y or
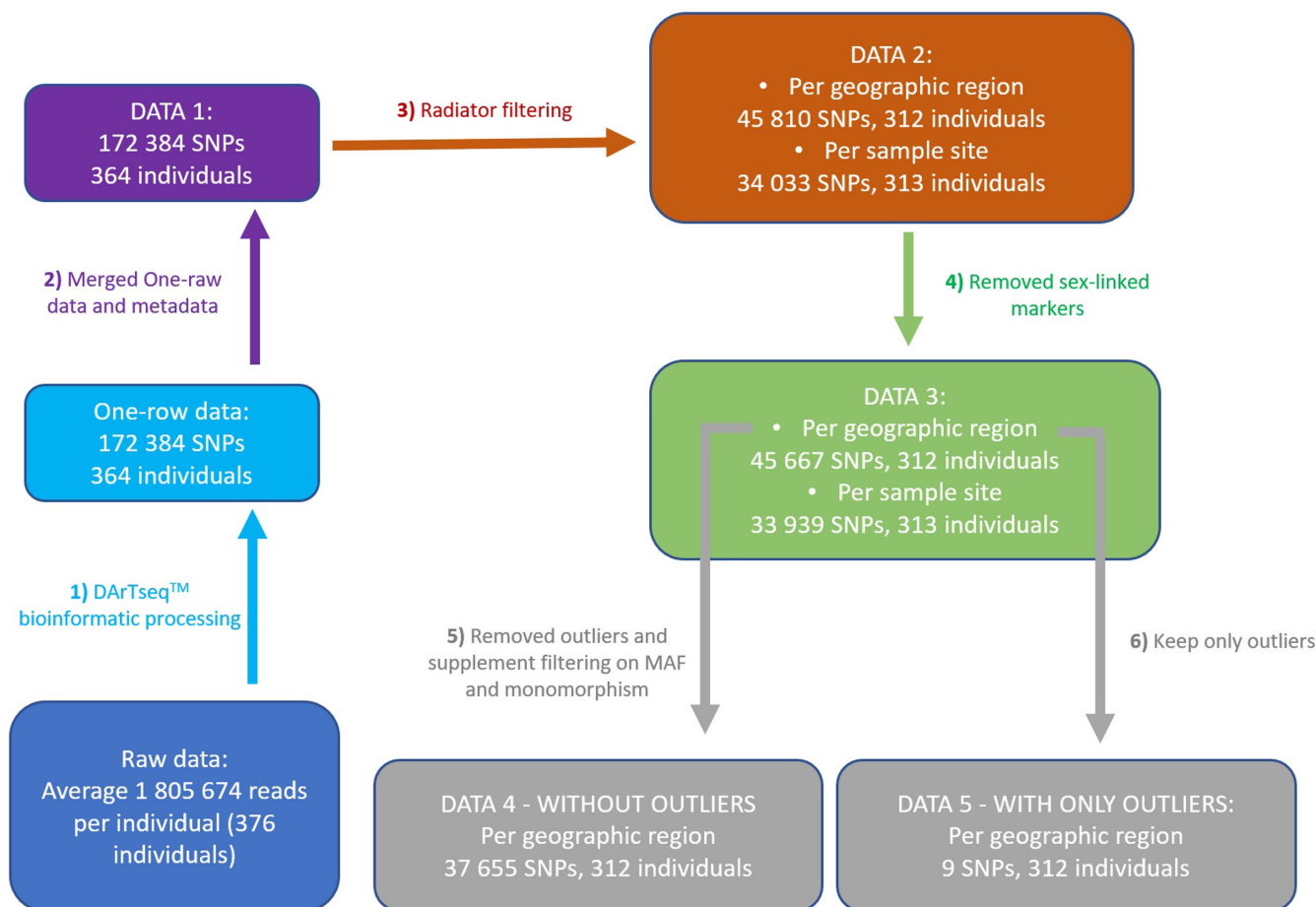
FIGURE 2 *Prionace glauca*. Summary of the genetic data filtering process from DArT-sequencing read output to the final genotype DATA sets (DATA 3, DATA 4 and DATA 5). In step 5, minor allele frequency is abbreviated as MAF.

W chromosomes by their presence in one sex, but absence in the other. Similarly, X- or Z-linked markers were detected based on the heterozygosity and coverage patterns between sexes. All identified sex-linked markers were eliminated from the DATA 2 data set to obtain a modified data set (DATA 3) containing all other loci (Figure 2, see Appendix S1 for details on sex-linked analysis). Markers on the Y or W chromosomes were used to assign the genetic sex to individuals with missing phenotypic sex.

Outlier identification

Two complementary algorithms were used to identify putative outliers: PCADAPT version 4.3.3 (Luu et al., 2017) and OUTFLANK version 0.2 (Whitlock et al., 2015). We removed the outliers detected by both PCADAPT and OUTFLANK from DATA 3 with individual samples grouped per geographical region. The last step of filtering consisted of removing SNP loci with overall allele frequency lower than 0.01 ("minor" allele frequency; MAF) using DARTR version 1.9.9 (Georges et al., 2018). Thus, we finally obtained the DATA 4 data set where we kept only nonoutlier loci, and the DATA 5 data set where we kept only outlier loci (Figure 2; Appendix S1).

All downstream analyses were run on DATA 3 with all loci including outliers (with individual samples grouped per geographical region or per sample sites), and on DATA 4 and DATA 5 with only

nonoutlier and only outlier loci, respectively (with individual samples grouped per geographical region) (Figure 2, see Results section and Appendix S1).

2.3 | Population genetic analysis

All group stratification from geographical regions (Figure 1), as Mediterranean merged and not, was tested in population genetic analysis (see Appendix S1). Indices of genetic diversity including heterozygosity, allelic richness (Ar), F_{IS} and their probabilities under the null hypothesis of HWE were estimated using the DIVERSITY package version 1.9.90 (Keenan et al., 2013).

Pairwise F_{ST} and average sample-pairwise differences together with their significance estimated by bootstrap resampling were obtained using the STRATAG version 2.5.01 (Archer et al., 2017) and STAMPP (Pembleton et al., 2013) packages. Principal component analysis (PCA) on allelic frequencies was run under ADEGENET version 2.1.5 (Jombart, 2008; Jombart & Ahmed, 2011). Discriminant analysis of principal components (DAPC; Jombart et al., 2010) was run using the ADEGENET package. Principal components were selected from cross-validation in DAPC according to the putative origin of individuals and with 1000 replicates (see Appendix S1 for more details). Based

on the retained discriminant functions, we inferred group membership probabilities to assess the extent of admixture in the inferred clusters.

We estimated the partition of molecular variance within individual samples, between individual samples from sample sites (or geographical regions), and between sample sites (or geographical regions) using an analysis of molecular variance (AMOVA; Excoffier et al., 1992) implemented in the R packages POPPR version 2.9.3 (Kamvar et al., 2014) and PEGAS version 1.1 (Paradis, 2010). To test for significance, we performed a randomization test. The matrices of samples were randomly permuted as described in Excoffier et al. (1992).

Hierarchical genetic clustering was done using ADMIXTURE version 1.3 (Alexander et al., 2009) assuming a number (K) of ancestral populations between two and six. The value of K with lowest associated error value was identified using the cross-validation procedure of ADMIXTURE. Then, the R package STOCKR version 1.0.74 (Foster, 2020) was used with K values (designed in STOCKR to correspond to a number of differentiated groups) from two to six and following the approach outlined in Foster et al. (2018), which has been designed to discriminate groups with no contemporary mixture, based on assignment probability.

The correlation between pairwise genetic (F_{ST} and Euclidean Edwards' distance) and geographical distances was tested using a Mantel test with 1000 permutations between individuals and geographical regions using the R packages *adegenet* and *ade4* version 1.7–18 (Bougeard & Dray, 2018; Chessel & Dufour, 2004; Dray et al., 2007; Dray & Dufour, 2007) on the data set without outlier only (DATA 4).

2.4 | Demographic analysis

We used the software GADMA (Genetic Algorithm for Demographic Model Analysis; Noskova et al., 2020) to rebuild the evolutionary trajectory of the two main genetic clusters detected from the previous analyses (see Results). Our main objective was the reconstruction of the past and recent demographic trends of these populations, considering the global conservation status of the blue shark. Besides, we also expected demographic reconstruction to allow a better understanding of the position of one particular geographical region (namely, South Africa or SAF) relative to the two detected clusters.

GADMA implements a global genetic algorithm and different existing "*engines*" of local optimization, such as δaδi (Gutenkunst et al., 2009), moments (Jouganous et al., 2017) or momi (Kamm et al., 2020), to simulate the expected joint allele-frequency spectrum (JAFS) from multiple populations under various demographic scenarios, and compare it with the observed JAFS. More precisely, the genetic algorithm implemented in GADMA enables us to delineate time structures (epochs) showing particular trends in effective population size (N_e) through time (e.g., linear or exponential growth or decline for a given period of time). A local optimization algorithm supports finer inference of demographic parameter values in those predefined structures. This favours the identification of the demographic scenario most likely to explain the observed genetic variation, even with limited a priori knowledge, implying the exploration of a wide parameter space.

First, we converted the DATA 4 data set in Variant Call Format (VCF file) using the function *genomic_converter* in RADIATOR (see Appendix S1). Then from these converted data, we built the observed JAFS by grouping individual samples according to the populations delineated from the previous structure and clustering analyses. However, considering the computational costs of the analysis of high-density JAFS, we subsampled the original JAFS using EASYSFS (https://github.com/isaacovercast/easySFS) to allow the analysis with realistic computing time and resources. EASYSFS builds the JAFS on this subset, while selecting the number of individual samples and variants needed to maintain the characteristics of the initial JAFS. The EASYSFS approach implies a subsampling that has an effect similar to the reduction of population sample size, still allowing a reasonable trade-off between data resolution and computational limitations (see Fraisse et al., 2018).

Thus, we ran demographic inferences using a JAFS with 50×50 cells, composed by 31,901 and 32,387 segregating sites for Northern (northern Atlantic Ocean and Mediterranean Sea) and Southern (Indian and southwestern Pacific oceans) populations, respectively. The population structure analysis revealed a clear differentiation of those two clusters of samples (see Results). Hereafter, this will be referred as the 2-population model. The predefined 2-population demographic scenario allowed for N_e of an ancestral population to vary, before that ancestral populations split into two daughter populations, with steady N_e variation allowed and continuous gene flow occurring during divergence. This, overall, corresponded to an isolation-with-migration (IM) model integrating N_e variations. This 2-population model relied on 12 parameters, nine of which were quantitative (Figure 3.1, Table 4). Three qualitative parameters described trends and dynamics in population effective size (constant, linear or exponential). Five quantitative parameters described the effective size of each population at the start and the end of each time period. Two quantitative parameters described bidirectional migration rates between the two daughter populations. Finally, two quantitative parameters described the duration of the different time periods, specifically before and after the split of the ancestral population.

The South African geographical region was excluded from the 2-population model, due to the inconsistent results obtained depending on the methods employed for detecting differentiation (see Results). Thus, we included SAF as a possible undetected third demographic entity in what we will be referred to, hereafter, as a 3-population demographic model. The 3-population model thus distinguished the South African, Northern and Southern sampling regions. In the 3-population model, we tested two tree models: (a) first tree model—the ancestral population was split into the Northern population and a common population made up of SAF and the Southern population, which was split later; and (b) second tree model—the ancestral population was split into a Southern population
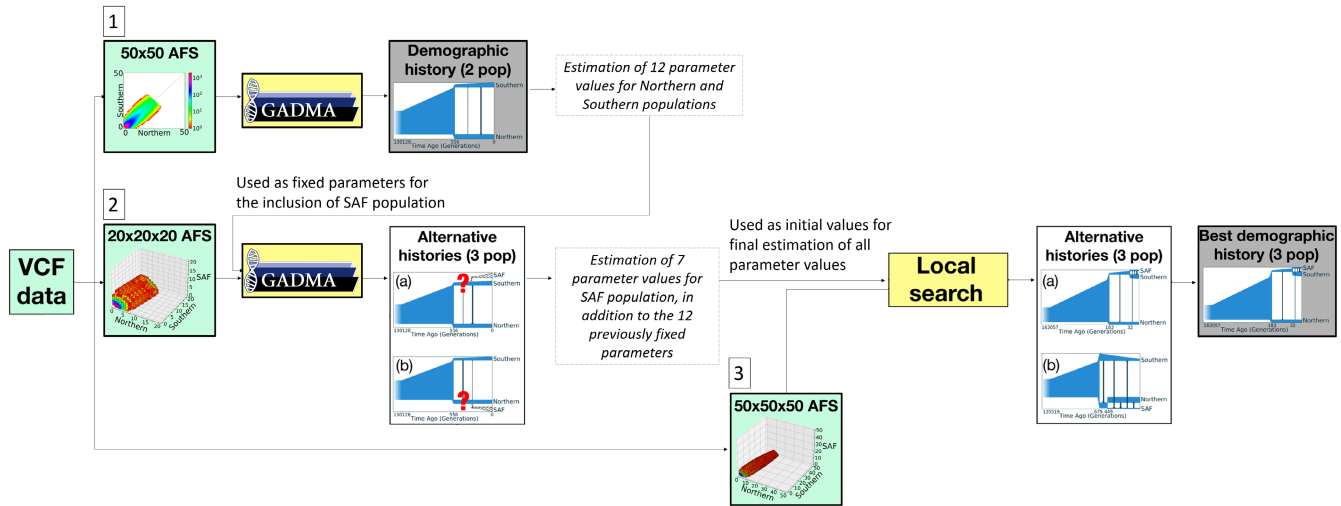
FIGURE 3 A scheme of demographic inference for two and three populations of the blue shark, *Prionace glauca*. The 2-population model (upper part, [1]) distinguished northern (Atlantic Ocean and Mediterranean Sea) from southern (Indian and southwestern Pacific oceans) populations. The 3-population models (middle and lower part, [2] and [3]) distinguished south African, northern (Atlantic Ocean and Mediterranean Sea) and southern (Indian and southwestern Pacific oceans) populations, with the two tree models differing depending on the late divergence of SAF from the northern (a) or southern (b) group. Light green colour corresponds to the data used (size and dimensions of the observed JAFS, obtained from DATA 4 converted into a VCF file). Light yellow refers to the algorithms used. White and grey refer to the evaluated scenarios, the latter representing the scenario identified as the most likely to explain the observed genetic variation.

and a common population made up of SAF and the Northern population, which was split later (Figure 3).

In a first step, all parameter values (both qualitative and quantitative) for the Northern and Southern populations were fixed as pointed in the 2-population models. Seven quantitative parameters related to the SAF geographical region were left to be inferred. Two were related to the effective population size of SAF at the beginning and at the end of its time period. One was related to its divergence time from either the "Southern (tree model (a))" or the "Northern (tree model (b))" population. Four were related to migration rates with the Northern and the Southern populations. For fast inference of those seven parameters, we used a downsized JAFS of $20 \times 20 \times 20$ cells obtained using EASYSFS (Figure 3.2).

In a further step, we re-estimated all parameters (16 of which were quantitative, Supporting Information S7) from the 3-population model using Powell's local search algorithm and a bigger JAFS of $50 \times 50 \times 50$ with 32,387, 31,901 and 31,557 segregating sites for Northern, Southern and SAF populations (Figure 3.3). Fixed and inferred parameter values from the previous step were used as initial points of the run.

For both the 2- and 3-population models, we converted the inferred parameter values into biologically meaningful values (i.e., genetic units), using a mutation rate (μ) of 10^{-8}—mutation rate reported on sequences in Pirog (2018) in concordance with the mutation rate on hammerhead shark (Duncan et al., 2006)—and the effective sequence length (L) of 2,598,195 bp as described in Rougeux and Bernatchez (2017). We first estimated the ancestral effective population size (N_{anc}) from flux theta (θ):

$$N_{anc} = \frac{\theta}{4\mu L} \#(1)$$

Then, we defined the effective population size of contemporary populations (N_i):

$$N_i = nu_i . N_{anc} \#(2)$$

where nu_i corresponds to the inferred effective population size for population i from the model. The migration rate (M) between populations (i and j) was estimated as the proportion of individuals per generation migrating from population j to population i:

$$M_{ij} = \frac{m_{ij}}{2N_{anc}} \#(3)$$

where m_{ij} corresponds to the migration parameter estimated from the model.

Finally, we converted time parameter values (i.e., duration of different epochs) in number of generations (t_i) and inferred the duration of divergence in years (T_i) by integrating a rounded generation time (t_g) of 9 years—as previously published estimates were 8.1 years (IOTC, 2007), and 8.2 and 9.8 years for South African and northern Atlantic populations, respectively (Cortés et al., 2015) (giving a mean generation time of 8.70–9 years):

$$T_i = t_i . t_g . 2N_{anc} \#(4)$$

For demographic inferences, we used 50 independent GADMA runs with the engine *moments* (Jouganous et al., 2017) to observe convergence in models and infer parameter values, as well as statistical robustness.

As all model parameter values were positive, their logarithms were used to calculate confidence intervals (CIs) for the inferred

parameter values. Each bootstrap was performed 100 times under the assumption that all SNPs are independent.

3 | RESULTS

3.1 | Samples

The body length of individuals ranged from 74.5 to 330.0 cm FL with a mean of 140.4 cm FL. Females were on average shorter than males (Appendix S1 and S2) but the opposite trend was observed in the northern Atlantic, western Indian Ocean and eastern Indian Ocean geographical regions (Appendix S1). The smallest individuals were sampled in the northern Atlantic and the largest in the Mediterranean Sea (Appendix S1). As only 23 of the 54 individuals sampled from the Mediterranean were measured, caution should be taken when interpreting these results on body size. A study with a three times higher sample size (https://fishreg. ec.europa.eu/web/medbluesgen/sampling-data) revealed a difference in the range of sizes between East and West Mediterranean samples.

3.2 | Sequencing and quality control

DArT sequencing yielded 545,764–2,702,952 reads per individual with an average of 1,805,674 (Figure 2). We obtained 364 genotypes and 172,384 SNPs after applying the DArTseq analytical pipeline (DATA 1; Figure 2). The different filtering steps using the R package RADIATOR (detailed in Appendix S1) resulted in a data set of 45,810 SNPs (one SNP per de novo assembled fragment) from 312 individuals when considering a stratification per geographical region (Filtration 1), and 34,033 SNPs from 313 individuals when considering a stratification per sample site (Filtration 2; DATA 2) (Figure 2; Appendix S1). Individual samples from the northeastern Pacific (NPAC, Hawaii) were discarded during this process, as NPAC consisted of only four individuals with high genotype missingness (considered as a potential result of long-term storage and low DNA quality). The next steps of filtering removed 143 sex-linked SNPs from DATA 2 when considering a stratification per geographical region (45,810 SNPs initially), and 94 sex-linked SNPs from DATA 2 when considering a stratification per sample site (34,033 SNPs initially). From this stage, further filtering led to identical results regardless of a stratification per sample sites or per geographical region, indicating robust data (Appendix S1). Thus, search for outliers from DATA 3 was performed considering a stratification per geographical region only (Filtration 1), and not per sample site. We detected nine outliers in common with both OUTFLANK and PCADAPT, 2832 loci that were monomorphic at this stage, and 5171 SNPs with allele frequency below 0.01, yielding to a final data set of 37,655 nonoutlier SNPs on a total of 312 individual samples (DATA 4) (Figure 2). Analyses on the nine outlier SNPs (DATA 5) revealed results very similar to those detailed below (but see section 3.4 for an exception

TABLE 1 Genetic diversity estimates for *Prionace glauca* per geographical region and without outliers (from DATA 4: 37,655 nonoutlier SNPs and 312 individuals).

Pop	Ar	Nb	H_O	H_E	H_E unbiased	F_{IS}	Test global HWE	Test significance HWE (homozygote deficiency)	Test significance HWE (heterozygote deficiency)
NATL	1.594 (1.54–1.62)	42	0.145	0.168	0.170	0.091 (0.074–0.088)	1.000	1.000	1.000
NEATL	1.568 (1.50–1.61)	21	0.142	0.166	0.170	0.102 (0.069–0.094)	1.000	1.000	1.000
MED	1.583 (1.53–1.61)	45	0.142	0.166	0.168	0.099 (0.083–0.096)	1.000	1.000	0.000
SAF	1.583 (1.53–1.60)	105	0.140	0.166	0.166	0.115 (0.103–0.113)	0.000	1.000	0.000
WIO	1.562 (1.49–1.60)	22	0.141	0.163	0.167	0.088 (0.059–0.081)	1.000	1.000	1.000
NIO	1.547 (1.48–1.60)	16	0.143	0.161	0.166	0.067 (0.028–0.057)	1.000	1.000	1.000
EIO	1.506 (1.44–1.58)	8	0.145	0.157	0.167	0.031 (−0.067–0.021)	1.000	1.000	1.000
SWPAC	1.581 (1.53–1.61)	53	0.139	0.166	0.167	0.113 (0.096–0.110)	0.000	1.000	0.000

Note: Allelic richness (Ar) with the low and high 95% CI, number of individual samples (Nb), observed heterozygosity (H_O), expected heterozygosity (H_E), unbiased expected heterozygosity (Nei 1978) (H_E unbiased), inbreeding coefficient (F_{IS}) with the low and high 95% CI on F_{IS}, p-values from a chi-square test for goodness-of-fit to Hardy–Weinberg equilibrium (HWE), testing significance of homozygote and heterozygote deficiency. MED, Mediterranean; NATL, northern Atlantic; NEATL, northeastern Atlantic; SAF, South Africa; EIO, eastern Indian Ocean; NIO, northern Indian Ocean; SWPAC, southwestern Pacific; WIO, western Indian Ocean.

in pairwise F_{ST} values). Thus, unless stated otherwise, in the section below, we focus on results from the DATA 4 data set including non-outlier SNPs with a stratification per geographical region. Results for analyses on other data sets or with a stratification per sample site are presented in Appendix S1.

Phenotypic and genetic sex assignment matched very well. Only 18 individuals were corrected out of the 215 individuals with phenotypic sex (nine male to female corrections and nine female to male corrections). These phenotypic identification errors in the data are probably due to human error. The few samples with an incorrect phenotypic sex were collected by fishermen without bringing the individual on board. In addition, at least one fisherman reversed the sex identification (female for male and vice versa).

3.3 | Diversity

Genetic diversity values are presented in Table 1 and Appendix S1. Heterozygosity was low in all geographical regions (observed around 14% and expected around 16%–17%). These levels of genetic diversity, very similar among all sampled area, are consistent with previous reports (Bailleul et al., 2018; Leone et al., 2017). We did not detect significant Hardy–Weinberg disequilibrium, except for South Africa and the southwestern Pacific (SWPAC) where observed heterozygosity was lower than expected. The positive F_{IS} values obtained (0.031–0.115) differed from zero in all areas except the Eastern Indian Ocean (EIO), possibly due to low statistical power linked to low sample size (N = 8).

3.4 | Genetic differentiation

Differences between geographical regions, between individual samples within a geographical region, and within individual samples explained 0.09%, 11.83% and 88.08% of the molecular variance, respectively. Although the ϕ statistic of population differentiation suggested a low amount of differentiation between geographical

regions (Appendix S1), the variance estimates within and between samples, and between geographical regions were all significant (p < .001).

Pairwise F_{ST} values were of the order of 10^{-3} to 10^{-4} both between geographical regions (Table 2) and between sampling sites (Table 3). F_{ST} values were significant among all geographical regions, with South African populations differentiated from the northern Atlantic but not from Indo-Pacific ones (Table 2), while no genetic differentiation was detected within regions (Table 3), with two exceptions involving the South African site SAF2 differing from SWPAC2 and SWPAC3 in the Indo-Pacific (Table 3). A similar pattern emerged on the data set containing only outlier loci and a stratification per geographical region (DATA 5) (F_{ST} Tables S12 and S13 from Appendix S2).

Clustering analyses using PCA (Appendix S1 and S3), DAPC (Figure 4), ADMIXTURE (Figure 5a; Appendix S1) and STOCKR (Figure 5b; Appendix S1) revealed two distinct genetic groups, one including geographical regions from the northern Atlantic and the Mediterranean (MED, NATL and NEATL), and the other including geographical regions from the Indo-West Pacific (EIO, NIO, WIO and SWPAC). Individual samples from the SAF geographical region showed an admixed profile with ADMIXTURE analysis, while STOCKR clustered SAF individuals with Indo-West Pacific ones (in concordance with F_{ST} results) with both "non-outlier" (DATA 4) and "outlier" (DATA 5) data sets.

Finally, no significant correlation between geographical and genetic distance (either expressed as pairwise F_{ST} or Euclidean distance) was detected through the Mantel test performed on geographical regions (p > .05) (Appendix S1).

3.5 | Demographic inference

3.5.1 | Scenario with northern and southern populations (2-population model)

The demographic scenario showing the best fit to the observed genetic variation (log-likelihood = −2054.75) (Figure 6; Supporting

TABLE 2 Pairwise F_{ST} values and their level of significance after correction with q-value (*p < .01, **p < .001) (from DATA 4: 37,655 nonoutlier SNPs and 312 individuals) per geographical region.

	MED (45)	NATL (42)	NEATL (21)	SAF (105)	EIO (8)	NIO (16)	WIO (22)	SWPAC (53)
MED		0.0007**	0.0010**	0.0015**	0.0023*	0.0017**	0.0017**	0.0022**
NATL			0.0005*	0.0012**	0.0010*	0.0011**	0.0016**	0.0017**
NEATL				0.0017**	0.0015*	0.0015**	0.0015**	0.0020**
SAF					0.0000	0.0000	0.0000	0.0000
EIO						0.0004	0.0000	0.0000
NIO							0.0000	0.0000
WIO								0.0001
SWPAC								

Abbreviations: EIO, eastern Indian Ocean; MED, Mediterranean; NATL, northern Atlantic; NEATL, northeastern Atlantic; NIO, northern Indian Ocean; SAF, South Africa; SWPAC, southwestern Pacific; WIO, western Indian Ocean.

TABLE 3 Pairwise F_{ST} values and their level of significance after correction with q-value (*p <.01, **p <.001) (from DATA 3: 33,939 SNPs and 313 individuals) per sampling site.

	NATL	NEATL	MED1	MED2	SAF1	SAF2	WIO	NIO	EIO	SWPAC1	SWPAC2	SWPAC3
	(33)	(20)	(29)	(14)	(14)	(76)	(20)	(15)	(7)	(30)	(10)	(9)
NATL												
NEATL	0.0005											
MED1	0.0004**	0.0008*										
MED2	0.0013**	0.0012**	0.0005									
SAF1	0.0014**	0.0015**	0.0015**	0.0028**								
SAF2	0.0021**	0.0025**	0.0019**	0.0036**	0.0001							
WIO	0.0022**	0.0024**	0.0021**	0.0036**	0.0002	0.0000						
NIO	0.0024**	0.0028**	0.0025**	0.0039**	0.0004	0.0003	0.0000					
EIO	0.0025*	0.0031**	0.0031**	0.0049**	0.0008	0.0008	0.0000	0.0007				
SWPAC1	0.0028**	0.0030**	0.0029**	0.0044**	0.0003	0.0002	0.0000	0.0002	0.0002			
SWPAC2	0.0030**	0.0032**	0.0032**	0.0046**	0.0006	0.0007*	0.0001	0.0000	0.0000	0.0000		
SWPAC3	0.0034**	0.0029**	0.0033**	0.0051**	0.0006	0.0012*	0.0000	0.0012	0.0006	0.0007	0.0000	

Abbreviations: EIO, eastern Indian Ocean; MED, Mediterranean; NATL, northern Atlantic; NEATL, northeastern Atlantic; NIO, northern Indian Ocean; SAF, South Africa; SWPAC, southwestern Pacific; WIO, western Indian Ocean (see Figure 1).

Information S4) corresponded to an ancestral population that started to linearly increase ~130,000 generations ago (between ~1 and 1.275 million years ago) reaching an effective population size of 30,000 to up to 170,000 individuals, before splitting into two populations (Figure 7). During the split that would have occurred ~550 generations ago (i.e., ~,000 [4503–5449] years ago), the two populations may have experienced important bottlenecks, as suggested by the inferred contemporary effective population sizes of only about 5300 and 6400 in Northern and Southern populations, respectively (Table 4). The constant effective population size of the Northern population was estimated to be ~5300 and the Southern population may have experienced a marginal linear growth of ~2000 (~4200 to ~6300) between the time of split and the present day. In addition, an important asymmetry in gene flow was estimated, with preferential migration from Southern to Northern population ($M_{Sou-Nor} = 0.168$ vs. $M_{Nor-Sou} = 0.004$) (Table 4).

3.5.2 | Scenario with northern and southern populations, and South Africa (3-population model)

A 3-population (Northern and Southern sampling regions, and South Africa) demographic model was constructed to evaluate the most likely membership of SAF individuals favoured in the first tree model (a) (i.e., with the SAF population originating from the Southern cluster) (Supporting Information S5–S8). Nevertheless, non-negligible exchange through migration was detected over time (Supporting Information S6 and S7) between the Northern and Southern clusters in particular, through SAF which seemingly acts as a stepping stone between the Atlantic and the Indo-West Pacific regions.

4 | DISCUSSION

In contrast to previous reports of large scale panmixia in the blue shark (within oceanic basins: Queiroz et al., 2012; King et al., 2015; and among oceanic basins: Verissimo et al., 2017; Ovenden et al., 2009; Taguchi et al., 2015; Bailleul et al., 2018), our results for the first time demonstrate clear evidence of population genetic structure both within and among oceanic basins. These patterns of population differentiation were obtained with genome-wide markers. This study also hints at a genetic bottleneck in the recent past.

4.1 | Genetic diversity, population structure and demographic history of blue shark

Levels of genetic diversity were consistent with previous reports on this species (Bailleul et al., 2018; Leone et al., 2017) and similar to those reported in the closely related genus *Carcharhinus* (Green et al., 2019; Momigliano et al., 2017; Pazmiño et al., 2017). The limited but significant heterozygote deficiency was comparable to results
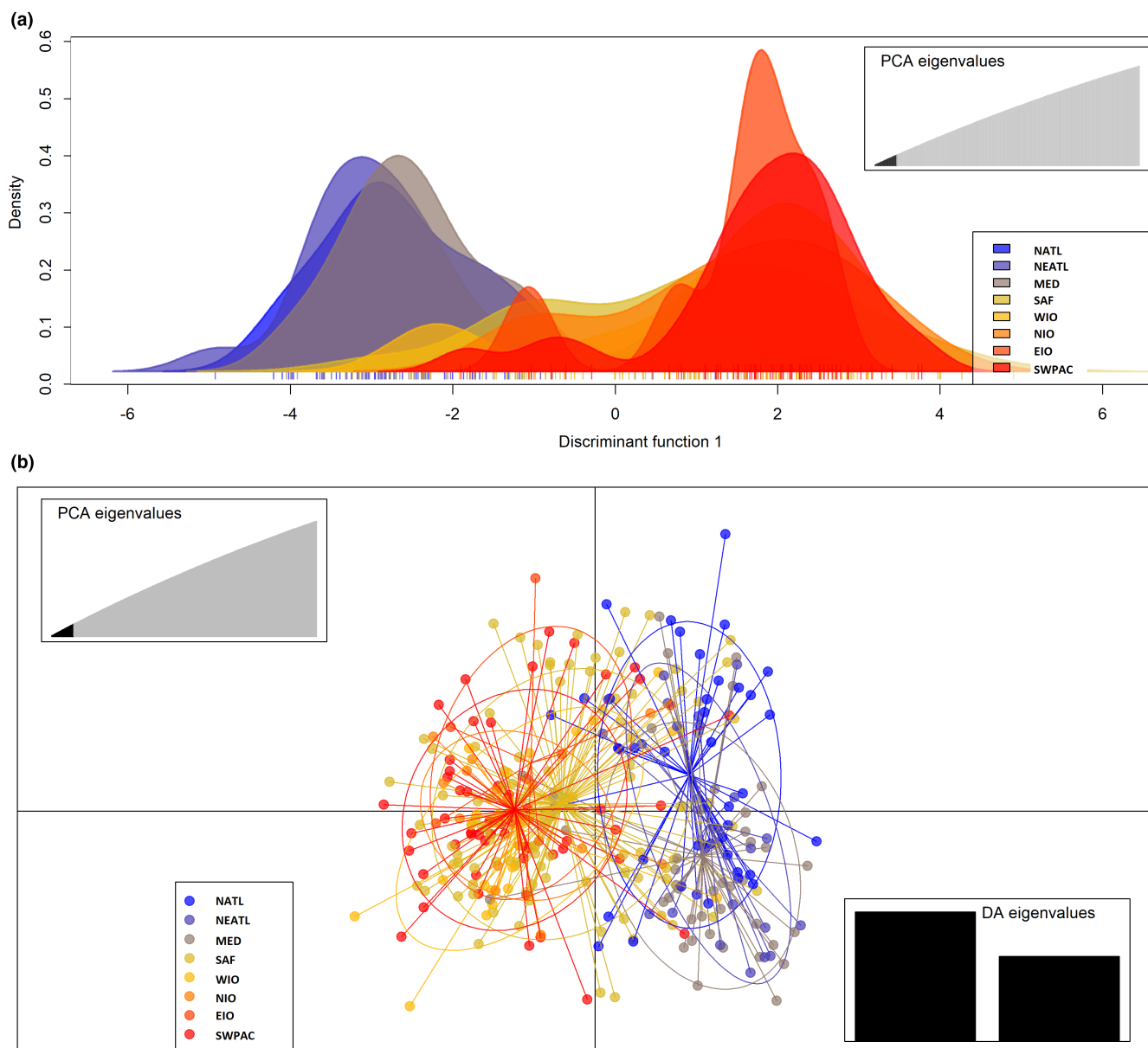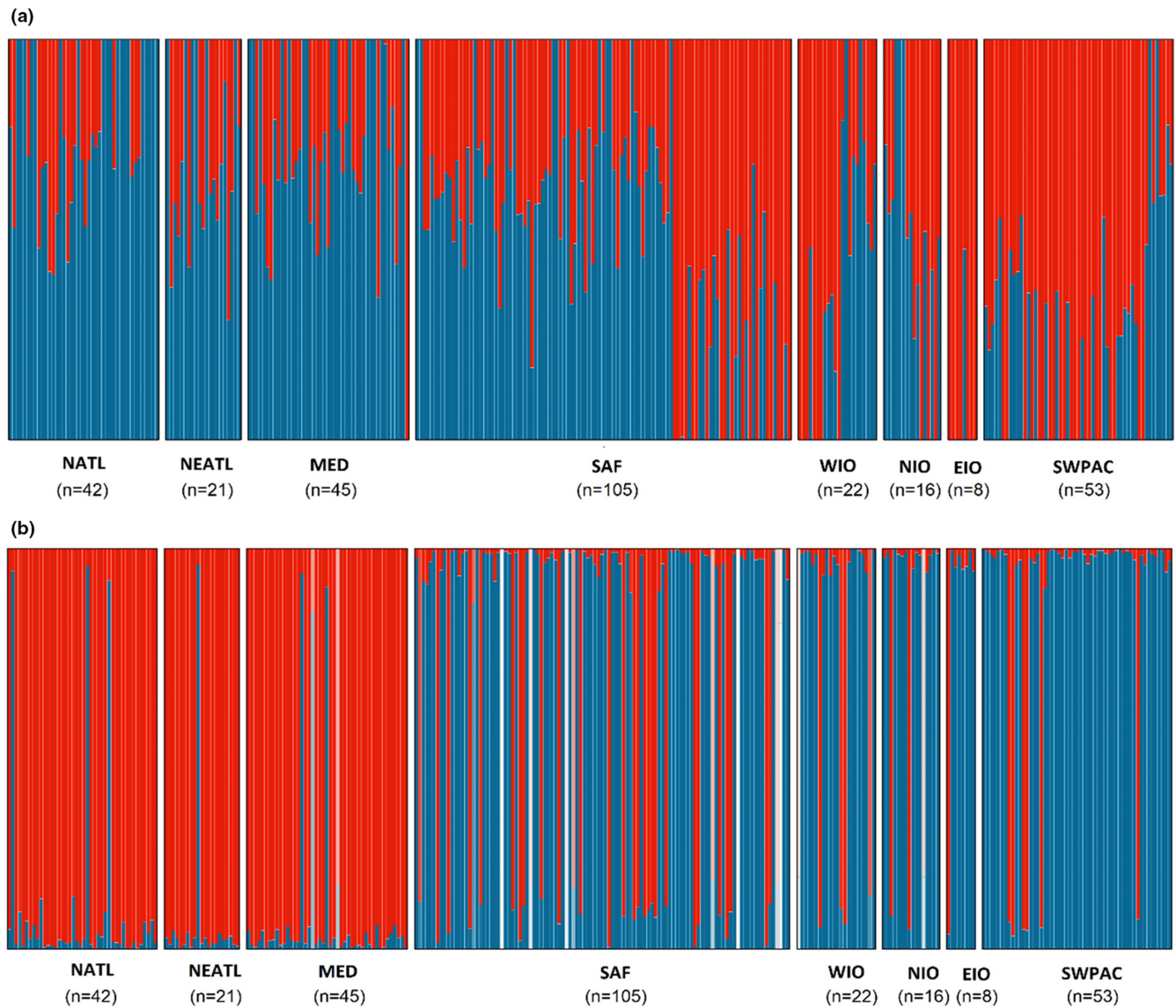
FIGURE 4 *Prionace glauca*. Results of genetic clustering using DAPC (from DATA 4: 37,655 nonoutlier SNPs and 312 individuals). (a) Density of individuals based on discrimination function with $K = 2$. (b) Scatter plot with $K = 3$, with colours corresponding to geographical regions. EIO, eastern Indian Ocean; MED, Mediterranean; NATL, northern Atlantic; NEATL, northeastern Atlantic; NIO, northern Indian Ocean; SAF, South Africa; SWPAC, southwestern Pacific; WIO, western Indian Ocean.

from previous studies (Bailleul et al., 2018; Verissimo et al., 2017). This is probably due to null alleles considering the absence of any behaviour known to favour inbreeding.

Significant pairwise F_{ST} values, together with genetic clustering analyses, revealed two distinct genetic clusters across the studied area: (i) the northern Atlantic Ocean region, including the Mediterranean Sea, and (ii) the Indo-West Pacific region; these seemingly acted as independent demographic units. In fact, most analyses here pointed toward a clear split between samples collected in the Mediterranean and northern Atlantic and other areas. There was also subtle differentiation between the Atlantic and the Mediterranean (significant F_{ST} values) when they were examined in more detail.

Reconstruction of past demographic history using the site frequency spectrum suggested that the two main clusters diverged from an ancestral population after it experienced a substantial increase in effective population size. Estimating the time periods of population growth for the ancestral population, as well as divergence time between ancestors of the contemporary populations, required us to postulate the average generation time. We chose 9 years as an intermediate value between the previous estimates of 8.1, 8.2 and 9.8 years (Cortés et al., 2015; IOTC, 2017). Under this scenario, the linear growth of the ancestral population would have started in the early Pleistocene, between 1.05 and 1.28 million years ago, and the split into Northern and Southern populations would have happened 4503–5449 years ago (~550 generations ago), during the Holocene.

-WILEY┤

(a)

(b)

FIGURE 5 *Prionace glauca*. Results of genetic clustering using ADMIXTURE (a) and STOCKR (b) (from DATA 4: 37,655 nonoutlier SNPs and 312 individuals). Individuals with admixed background are indicated in white, as STOCKR does not test admixture. EIO, eastern Indian Ocean; MED, Mediterranean; NATL, northern Atlantic; NEATL, northeastern Atlantic; NIO, northern Indian Ocean; SAF, South Africa; SWPAC, southwestern Pacific; WIO, western Indian Ocean.

Palaeoclimatic events could have triggered the divergence between Northern and Southern populations: Holocene tropical sea-surface temperatures (SSTs) followed a warming trend until 5000 years ago and a global stabilization until the present, albeit with some local variations. Leduc et al. (2010) revealed a warming of up to ~2°C (SSTs) in the western tropical Atlantic and eastern tropical Pacific from the early Holocene to the present. Meanwhile, a global Northern Hemisphere cooling happened about 5000 years ago (Masson-Delmotte et al., 2013). Lake sediment records from Greenland "suggest that around 4,500 and 650 years ago variability associated with the North Atlantic Oscillation changed from generally positive to variable, intermittently negative conditions" (Masson-Delmotte et al., 2013; Olsen et al., 2012). Furthermore, this lowering of SST occurred concomitantly in the Southern Hemisphere. In the Australian–New Zealand region, Holocene SST followed a cooling

trend (Bostock et al., 2013), as in the high-latitude Southern Ocean from the early to the late Holocene (Kaiser et al., 2008; Shevenell et al., 2011). These past variations in SST may have favoured a split between Northern and Southern populations. Shifts in blue shark reproductive seasons between the two hemispheres might have contributed to maintain that scission. In fact, while reproduction occurs in the summer (July, August) in the Northern Hemisphere (Fujinami et al., 2017), it is reported as more likely from December to July in the southwestern equatorial Atlantic Ocean (Coelho et al., 2017), and from October to December in the Indian Ocean (Druon et al., 2022).

Historical demography analysis suggested that this past divergence event was associated with a strong bottleneck followed by rather constant population size in both the Northern and Southern populations, despite an increase (albeit moderate) of the latter. The
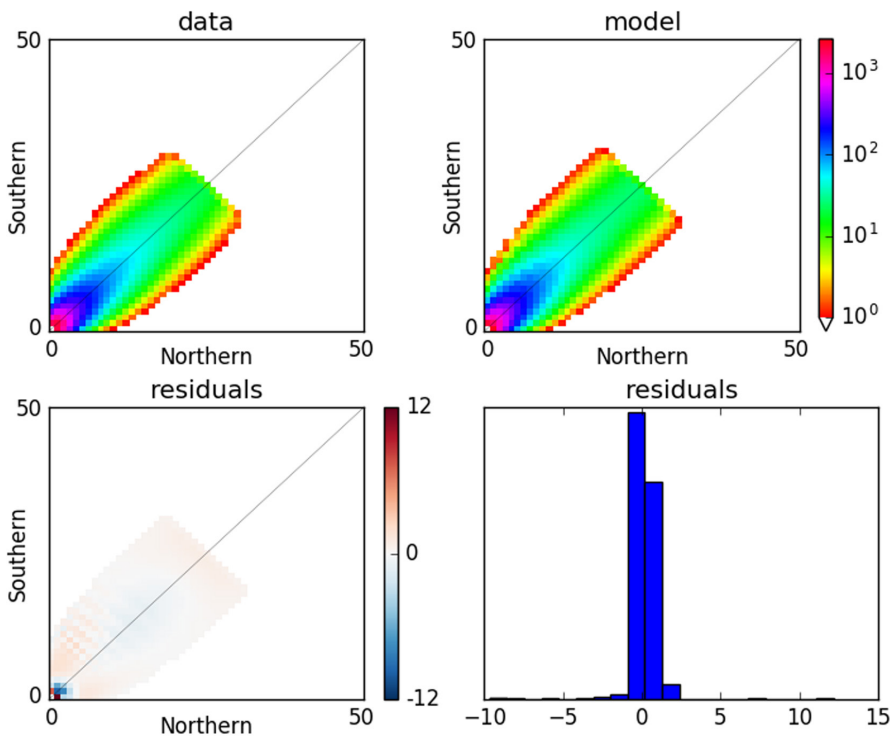
FIGURE 6 Projection of the joint allele frequency spectrum (JAFS) observed from empirical data (top left) (50×50 cells JAFS subsampled from DATA 4—37,655 nonoutlier SNPs and 312 individuals), and expected under the best demographic scenario inferred by GADMA (top right). The bottom line represents the Anscombe residuals (left) and the histogram of the residuals (right) from the comparisons between the observed and expected JAFS.
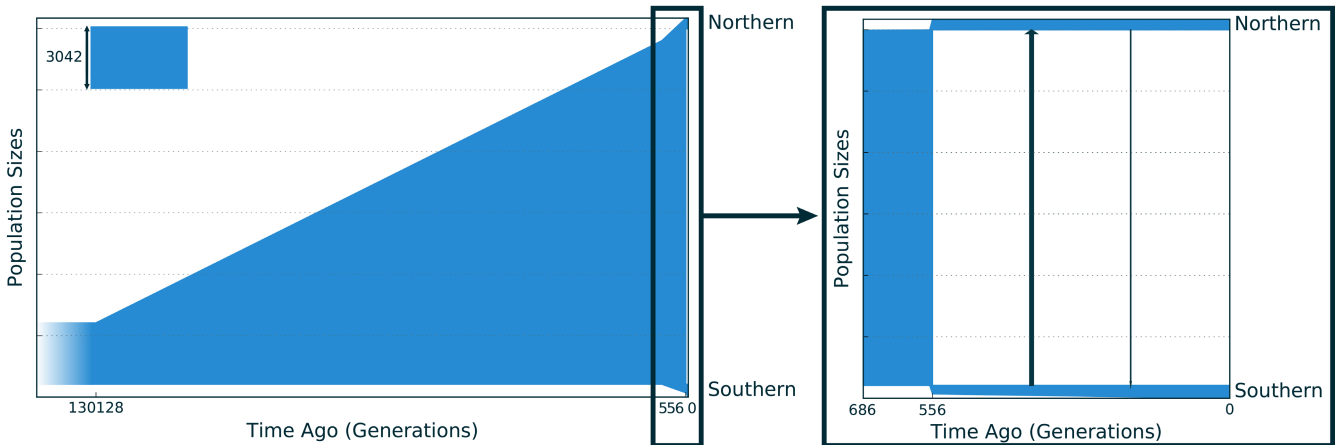
FIGURE 7 Schematic plot of the best demographic scenario inferred by GADMA for the demographic history of southern and northern populations. Past time is measured in number of generations, zero generation being the present time. Vertical arrows in the right panel represent asymmetric migration after the split.

GADMA analysis suggested that just after the split, the effective population size of both daughter populations represented only ~2% to 3% of the ancestral effective population size. Furthermore, the analysis suggested rather low contemporary effective population sizes ($N_e \sim 4000$–6500 based on the 2-population model). These estimates are of the same order of magnitude as the estimates (~4000–5000) previously proposed by Verissimo et al. (2017) in the Atlantic, and King et al. (2015) in the Pacific, using distinct estimation methods based on microsatellite genotype data. Historical demography analysis also suggested limited and strongly asymmetric gene flow, most of it being directed from the Southern population to the Northern population. This asymmetrical direction of gene flow might be

due to the increase in population size of the Southern population (e.g., Rougeux & Bernatchez, 2017). Besides, gene flow toward the Northern area might explain the difficult assignment of the individual samples from the South African (SAF) region to one or the other of the two genetic clusters detected by clustering analysis.

In fact, the position of the SAF samples relative to the two clusters slightly varied among genetic clustering methods. For instance, PCA and ADMIXTURE analyses suggested an intermediate position of the SAF sample between the Atlantic and the Indo-West Pacific. In contrast, STOCKR (designed to explicitly ignore historical admixture) and F_{ST} values pointed toward the inclusion of the SAF samples in the Southern cluster, in line with the 3-population GADMA demographic

TABLE 4 Demographic parameter values inferred by GADMA from a 50×50 JAFS with the 2-population model including northern (northern Atlantic Ocean and Mediterranean Sea) and southern (Indian and southwestern Pacific oceans) populations.

Parameter	Value	CI	Unit	Parameter definition
N_{anc}	30,422	[12,745–29,119]	Individuals	Population size of the ancestral population
N_{A_split}	176,072	[152,916–172,826]	Individuals	Population size of the ancestral population after linear growth
N_{Nor0}	5255	[1315–7144]	Individuals	Population size of the Northern population now after linear growth
N_{Nor}	5255	[1315–7144]	Individuals	Population size of the Northern population after the split and until now (constant size from N_{Nor0})
N_{Sou0}	4220	[979–7382]	Individuals	Population size of the Southern population after split of the ancestral population
N_{Sou}	6356	[1067–10,171]	Individuals	Population size of the southern population now after linear growth
T_A	130,128	[141,491–197,366]	Number of generations	Time of the start of ancestral population linear growth
T_{split}	556	[139–705]	Number of generations	Time of ancestral population split
$M_{Sou-Nor}$	0.0168	[0.0127–0.0853]	Proportion per generation	Migration rate from Southern population to Northern population
$M_{Nor-Sou}$	0.0004	[0.0001–0.0173]	Proportion per generation	Migration rate from Northern population to Southern population

Abbreviations: CI, confidence interval; $M_{Nor-Sou}$, migration rate from Northern to Southern population; $M_{Sou-Nor}$, migration rate from Southern to Northern population; N_{A_split}, population size after the initial split; N_{anc}, ancestral population size; N_{Nor}, population size of the Northern population after the split; N_{Nor0}, present population size of the Northern population; N_{Sou}, population size of the Southern population after the split; N_{Sou0}, present population size of the Southern population; T_A, start time of ancestral population growth; T_{split}, time from the initial split.

analysis. Yet, F_{ST} values also suggested genetic differentiation between the southwestern Atlantic and the Indo-West Pacific, similar to earlier reports using mitochondrial DNA markers (Bitencourt et al., 2019). The South African region might be an area of occasional reproductive mixing between the northern and southern populations or it might be under the influence of an east–west migration road (mix of individuals). Indeed, in this region, oceanic currents are particularly strong and form eddies. Off the southern tip of Africa, the Agulhas current retroflects eastward into the Indian Ocean. This retroflection takes the form of an unstable jet that can shed warm eddies into the Atlantic Ocean (Nikolic et al. 2020b). Studies on bigeye tuna reported a lack of a clear physical barrier preventing mutual exchange between the Atlantic and Indo-West Pacific regions and the co-occurrence of two separate populations off the southern tip of Africa (Chow et al., 2000; Durand et al., 2005). Tagging data on yellowfin tuna revealed the migration of individuals from the western equatorial Indian Ocean to the southern Benguela region off western South Africa (Eveson et al., 2015; Murua et al., 2015). Previous studies on cosmopolitan large pelagic sharks in particular (e.g., Bester-van der Merwe et al., 2017; Portnoy et al., 2010), and other cosmopolitan large pelagic bony fishes in general (e.g., Mullins & Shaw, 2018; Nikolic et al. 2020b), also found similar population structure patterns and pointed to the potential role of the South African region in connecting populations from the Atlantic and Indian oceans.

It is unclear whether the differentiation detected between the two main clusters reflects a Northern–Southern split (possibly due to the shift in reproductive season between the two hemispheres: Nakano & Seki, 2003; Nakano & Stevens, 2008), or a split between the Mediterranean–Atlantic and Indo-West Pacific regions.

Characterizing additional samples from the southwestern Atlantic including the Brazilian samples discussed by Verissimo et al. (2017) and Bitencourt et al. (2019), and the southeastern Atlantic, such as Gulf of Guinea, might help to ascertain the localization and the origin of the split between the two main clusters identified here.

Despite this apparent split dominating the clustering analysis, our results also revealed structure at a finer spatial scale, with differentiation between the Mediterranean and the northern Atlantic. These results confirm previous suggestions of a differentiated Mediterranean population based on mitochondrial (Leone et al., 2017) and microsatellite data (Bailleul et al., 2018). Our results thus support the existence of two demographic units in the Northern Hemisphere (North Atlantic and Mediterranean), although this differentiation is subtler and less marked than the split between the two main clusters. This is also the case for swordfish, and the ICCAT considers the North Atlantic and the Mediterranean populations as two separate fish stocks (Greig et al., 1999). Furthermore, ongoing analyses with more samples of blue shark by A. Leone et al. (in prep.) will help investigate connectivity between the northeast Atlantic and the Mediterranean Sea.

4.2 | Implications for fisheries

Fisheries management requires the identification of demographically independent units (Carvalho & Hauser, 1995; Waples et al., 2008). Using simulations, Bailleul et al. (2018) showed the extensive time lag between demographic change and its detectable imprint in population genetic structure (the "grey zone" effect), and suggested that genome scans may offer the necessary power

to detect patterns of population structure and escape this "grey zone" effect. The results obtained here support this prediction, showing that denser locus coverage enables the detection of subtle genetic differences among blue shark populations from distinct ocean basins. They support the use of genome scans as a useful tool to define management units and assess demographic trends for conservation proposes. The ICCAT provided recommendations to fill gaps in our understanding of population differentiation using genetic data (ICCAT, 2015, 2019). The present results should feed future models and management plans by the ICCAT, particularly regarding the minimum number of management units to be considered. In fact, genetic differentiation between blue shark from the Mediterranean and the northern Atlantic indicates the occurrence of at least two independent demographic entities, supporting the need for a revision of the management units recognized thus far. We failed to detect very recent bottlenecks (i.e., less than 10 generations ago) using the GADMA analysis: the detection of such recent events is complex and varies depending on the type of genetic data and approaches (Sovic et al., 2019).

No genetic differentiation was detected between the Indian Ocean and the southwestern Pacific, which is consistent with tagging results that reveal long migrations by individuals from the southwestern Pacific, across the Indian Ocean to South Africa (West et al., 2004). Our easternmost samples came from southeastern Australia, New Zealand and New Caledonia: an additional eastern boundary of the Indian Ocean blue shark stock could be set at 170° E to also joint assessment across the Indian Ocean and southwest Pacific. A complementary assessment would require joint effort between the Indian Ocean Tuna Commission (IOTC) and the Western and Central Pacific Fishery Commission. In the Indian Ocean, the IOTC blue shark assessment currently assumes a single stock (IOTC, 2017). Although our results did not provide evidence for multiple stocks at the scale of the Indian Ocean, this lack of evidence for demographic independence within the Indian Ocean and between the Indian Ocean and the southern Pacific should still be interpreted cautiously considering the low number of migrants sufficient to erase population differentiation (Bailleul et al., 2018).

We encourage additional genetic studies including more locations, with a focus on the southern Atlantic, and the southeastern, central and northern Pacific, to refine our understanding of connectivity within the Indian Ocean and around South Africa. More importantly, considering the possible implication of difference in reproductive period among locations, we recommend targeted sampling in reproductive zones. Such additional data would help ascertain genetic differentiation among oceanic basins, and possibly detect finer-scale differentiation. Moreover, we recommend population monitoring within blue shark management units. Indeed, an anthropogenically driven decrease in blue shark effective population sizes could actually be occurring at present, but remain undetected. Such a phenomenon would be worthy of interest, considering the relatively low effective population sizes estimated in this study.

5 | CONCLUSION

Knowledge of population structure, dynamics and connectivity is essential for the management and conservation of exploited and threatened species. Indirect methods are a valuable source of information in most cases where information cannot be obtained through direct observations, a situation exemplified in the marine realm. Great expectations emerged with the availability of molecular markers enabling the estimation of geographical structure and demographic trends in the theoretical framework of population genetics, yet results have sometimes been inconclusive, particularly for those species with large population sizes and/or potential for large-scale migration. The results obtained here support Bailleul et al.'s (2018) prediction that the "grey zone effect" may be circumvented thanks to the enhanced power offered by genome scans. The use of several tens of thousands of SNPs enabled the detection of weak levels of population differentiation, demonstrating for the first time the existence of distinct demographic units in the blue shark. It also enabled the reconstruction of past fluctuations in effective population size. The present results should lead to a reconsideration of the definition of unit stocks for regional stock assessment in the blue shark and taking additional management measures (ex. joint assessment across the Indian and Pacific oceans) in the dedicated fisheries commissions. They should also stimulate dedicated genetic sampling of reproductive aggregations, rather than opportunistic sampling through fisheries, in still poorly represented areas of the blue shark's global range. Beyond the blue shark case, our results highlight the value of the increased power of genome scans to describe demographically independent populations and stocks. For those marine species in which the "population grey zone" has thus far hampered such essential discrimination, genome scans could help distinguish between true panmixia and insufficient statistical power from limited molecular markers.

the manuscript. All authors (Natacha Nikolic, Floriaan Devloo-Delva, Diane Bailleul, Ekaterina Noskova, Clément Rougeux, Chrystelle Delord, Cathy Liautard-Haag, Mohamad Hassan, Amandine D. Marie, Philippe Borsa, Pierre Feutry, Peter Grewe, Chrystelle Delord, Jessica Farley, Daniel Fernando, Sebastian Biton-Porsmoguer, François Poisson, Denham Parker, Agostino Leone, Jorden Aulich, Matt Lansdell, Francis Marsac and Sophie Arnaud-Haond) reviewed the manuscript.

CONFLICT OF INTEREST

The authors have no conflicts of interest.

OPEN RESEARCH BADGES

This article has earned an Open Data badge for making publicly available the digitally-shareable data necessary to reproduce the reported results. The data is available at [insert provided URL from Open Research Disclosure Form].

DATA AVAILABILITY STATEMENT

Metadata, raw data and final data are freely available from the IFREMER Sextant repository: https://sextant.ifremer.fr/record/f0ad76a4-a9d3-4cd7-aaf5-7a1a43dc1e99/ or https://sextant.ifremer.fr/Donnees/Catalogue#/metadata/f0ad76a4-a9d3-4cd7-aaf5-7a1a43dc1e99

AUTHORIZATIONS

Permit: 0001500212. This permit was issued under Biosecurity Act 2015 Section 179 (1).

ORCID

Natacha Nikolic https://orcid.org/0000-0002-6055-0923
Floriaan Devloo-Delva https://orcid.org/0000-0002-6757-2949
Chrystelle Delord https://orcid.org/0000-0002-2951-1272
Amandine D. Marie https://orcid.org/0000-0003-1212-1742
Pierre Feutry https://orcid.org/0000-0001-8492-5382

REFERENCES

Aires-da-Silva, A. M., Hoey, J. J., & Gallucci, V. F. (2008). A historical index of abundance for the blue shark (*Prionace glauca*) in the western North Atlantic. *Fisheries Research*, *92*, 41–52.

Aires-da-Silva, A. M., Maunder, M. N., Gallucci, V. F., Kohler, N. E., & Hoey, J. J. (2009). A spatially structured tagging model to estimate movement and fishing mortality rates for the blue shark (*Prionace glauca*) in the North Atlantic Ocean. *Marine and Freshwater Research*, *60*, 1029–1043.

Alexander, D. H., Novembre, J., & Lange, K. (2009). Fast model-based estimation of ancestry in unrelated individuals. *Genome Research*, *19*, 1655–1664.

Allaire, J. J., Xie, Y., McPherson, J., Luraschi, J., Ushey, K., Atkins, A., Wickham, H., Cheng, J., Chang, W., & Iannone, R. (2020). *Rmarkdown: Dynamic documents for R.* https://github.com/rstudio/rmarkdown

Archer, F. I., Adams, P. E., & Schneiders, B. B. (2017). Stratag: An r package for manipulating, summarizing and analysing population genetic data. *Molecular Ecology Resources*, *17*, 5–11.

Bailleul, D., Mackenzie, A., Sacchi, O., Poisson, F., Bierne, N., & Arnaud-Haond, S. (2018). Large-scale genetic panmixia in the blue shark (*Prionace glauca*): A single worldwide population, or a genetic lag-time effect of the "grey zone" of differentiation? *Evolutionary Applications*, *11*, 614–630.

Baum, J. K., & Blanchard, W. (2010). Inferring shark population trends from generalized linear mixed models of pelagic longline catch and effort data. *Fisheries Research*, *102*, 229–239.

Bester-van der Merwe, A. E., Bitalo, D., Cuevas, J. M., Ovenden, J., Hernández, S., da Silva, C., McCord, M., & Roodt-Wilding, R. (2017). Population genetics of southern hemisphere tope shark (Galeorhinus galeus): Intercontinental divergence and constrained gene flow at different geographical scales. *PLoS One*, *12*(9), e0184481.

Bitencourt, A., Silva, D. A., Carvalho, E. F., Loiola, S., & Amaral, C. R. L. (2019). Study of genetic variability of the blue shark *Prionace glauca* (Linnaeus, 1758). *Forensic Science International Genetics Supplement Series*, *7*, 594–596.

Biton-Porsmoguer, S. (2017). Análisis de la explotación del pez espada *Xiphias gladius* y de la tintorera *Prionace glauca* por la flota palangrera catalana durante el periodo 2010-2015 en el Mediterráneo occidental. *Revista de Biología Marina y Oceanografía*, *52*(1), 175–179.

Biton-Porsmoguer, S. (2018). Explotación intensiva de la tintorera *Prionace glauca* y del marrajo *Isurus oxyrinchus* en el Atlántico noreste entre 2001 y 2016. *Revista de Biología Marina y Oceanografía*, *53*(1), 27–38.

Biton-Porsmoguer, S., & Lloret, J. (2018). Potentially unsustainable fisheries of a critically-endangered pelagic shark species: The case of the blue shark (*Prionace glauca*) in the Western Mediterranean Sea. *Cybium: International Journal of Ichthyology*, *42*(3), 299–302.

Bostock, H. C., Barrows, T. T., Carter, L., Chase, Z., Cortese, G., Dunbar, G. B., Ellwood, M., Hayward, B., Howard, W., Neil, H. L., Noble, T. L.,

Mackintosh, A., Moss, P. T., Moy, A. D., White, D., Williams, M. J. M., & Armand, L. K. (2013). A review of the Australian–New Zealand sector of the Southern Ocean over the last 30 ka (Aus-INTIMATE project). *Quaternary Science Reviews*, *74*, 35–57.

Bougeard, S., & Dray, S. (2018). Supervised multiblock analysis in R with the ade4 package. *Journal of Statistical Software*, *86*, 1–17.

Campana, S. E., Joyce, W., & Manning, M. J. (2009). Bycatch and discard mortality in commercially caught blue sharks *Prionace glauca* assessed using archival satellite pop-up tags. *Marine Ecology Progress Series*, *387*, 241–253.

Campana, S. E., Marks, L., Joyce, W., & Kohler, N. E. (2006). Effects of recreational and commercial fishing on blue sharks (*Prionace glauca*) in Atlantic Canada, with inferences on the North Atlantic population. *Canadian Journal of Fisheries and Aquatic Sciences*, *63*, 670–682.

Carvalho, F., Ahrens, R., Murie, D., Bigelow, K., Aires-Da-Silva, A., Maunder, M. N., & Hazin, F. (2015). Using pop-up satellite archival tags to inform selectivity in fisheries stock assessment models: A case study for the blue shark in the South Atlantic Ocean. *ICES Journal of Marine Science*, *72*, 1715–1730.

Carvalho, G. R., & Hauser, L. (1995). Molecular genetics and the stock concept in fisheries. In G. R. Carvalho & T. J. Pitcher (Eds.), *Molecular genetics in fisheries* (pp. 55–79). Springer.

Chessel, D., & Dufour, A. T. (2004). The ade4 package – I: One-table methods. *R News*, *4*, 5–10.

Chow, S., Okamoto, H., Miyabe, N., Hiramatsu, K., & Barut, N. (2000). Genetic divergence between Atlantic and Indo-Pacific stocks of bigeye tuna (*Thunnus obesus*) and admixture around South Africa. *Molecular Ecology*, *9*, 221–227.

Clarke, S. C., Harley, S. J., Hoyle, S. D., & Rice, J. S. (2013). Population trends in Pacific oceanic sharks and the utility of regulations on shark finning. *Conservation Biology*, *27*, 197–209.

Clarke, S. C., Magnussen, J. E., Abercrombie, D. L., McAllister, M. K., & Shivji, M. S. (2006). Identification of shark species composition and proportion in the Hong Kong shark fin market based on molecular genetics and trade records. *Conservation Biology*, *20*, 201–211.

Coelho, R., Mejuto, J., Domingo, A., Yokawa, K., Liu, K. M., Cortés, E., Romanov, E. V., da Silva, C., Hazin, F., Arocha, F., Mwilima, A. M., Bach, P., Ortiz de Zárate, V., Roche, W., Lino, P. G., García-Cortés, B., Ramos-Cartelle, A. M., Forselledo, R., Mas, F., … Santos, M. N. (2017). Distribution patterns and population structure of the blue shark (*Prionace glauca*) in the Atlantic and Indian oceans. *Fish and Fisheries*, *19*(1), 90–106. https://doi.org/10.1111/faf.12238

Compagno, L. J. V. (1984). FAO species catalogue. Vol. 4. Sharks of the world. An annotated and illustrated catalogue of shark species known to date. Part 2. Carcharhiniformes. *FAO Fisheries Synopsis*, *4*, 655. http://www.fao.org/3/ad123e/ad123e00.htm

Cortés, E., Domingo, A., Miller, P., Forselledo, R., Mas, F., Arocha, F., Campana, S., Coelho, R., Da Silva, C., Hazin, F. H. V., Holtzhausen, H., Keene, K., Lucena, F., Ramirez, K., Santos, M. N., Semba-Murakami, Y., & Yokawa, K. (2015). Expanded ecological risk assessment of pelagic sharks caught in Atlantic pelagic longline fisheries. *Collective Volume of Scientific Papers ICCAT*, *1*, 2637–2688.

Cramer, J., Bertolino, A., & Scott, G. P. (1997). Estimates of recent shark bycatch by U.S. vessels fishing for Atlantic tuna and tuna-like species. *ICCAT Working Document* SCRS/97/58, *48*(3), 117–128.

da Silva, C., Kerwath, S. E., Wilke, C. G., Meyer, M., & Lamberth, S. J. (2010). First documented southern transatlantic migration of a blue shark *Prionace glauca* tagged off South Africa. *African Journal of Marine Science*, *32*, 639–642.

Davey, J. W., & Blaxter, M. L. (2010). RADSeq: Next-generation population genetics. *Briefings in Functional Genomics*, *9*, 416–423.

Dray, S., & Dufour, A. (2007). The ade4 package: Implementing the duality diagram for ecologists. *Journal of Statistical Software*, *22*, 1–20.

Dray, S., Dufour, A., & Chessel, D. (2007). The ade4 package – II: Two-table and K-table methods. *R News*, *7*, 47–52.

Druon, J.-N., Campana, S., Vandeperre, F., Hazin, F. H. V., Bowlby, H., Coelho, R., Queiroz, N., Serena, F., Abascal, F., Damalas, D., Musyl, M., Lopez, J., Block, B., Afonso, P., Dewar, H., Sabarros, P. S., Finucci, B., Zanzi, A., Bach, P., … Travassos, P. (2022). Global-scale environmental niche and habitat of blue shark (*Prionace glauca*) by size and sex: A pivotal step to improving stock management. *Frontiers in Marine Science*, *9*, 828412.

Duncan, K. M., Martin, A. P., Bowen, B. W., & De Couet, H. G. (2006). Global phylogeography of the scalloped hammerhead shark (Sphyrna lewini). *Molecular Ecology*, *15*(8), 2239–2251.

Durand, J.-D., Collet, A., Chow, S., Guinand, B., & Borsa, P. (2005). Nuclear and mitochondrial DNA markers indicate unidirectional gene flow of Indo-Pacific to Atlantic bigeye tuna (*Thunnus obesus*) populations, and their admixture off southern Africa. *Marine Biology*, *147*, 313–322.

Estes, J. A., Terborgh, J., Brashares, J. S., Power, M. E., Berger, J., Bond, W. J., Carpenter, S. R., Essington, T. E., Holt, R. D., Jackson, J. B. C., Marquis, R. J., Oksanen, L., Oksanen, T., Paine, R. T., Pikitch, E. K., Ripple, W. J., Sandin, S. A., Scheffer, M., Schoener, T. W., … Wardle, D. A. (2011). Trophic downgrading of planet earth. *Science*, *333*, 301–306.

Eveson, J. P., Hobday, A. J., Hartog, J. R., Spillman, C. M., & Rough, K. M. (2015). Seasonal forecasting of tuna habitat in the great Australian bight. *Fisheries Research*, *170*, 39–49.

Excoffier, L., Smouse, P. E., & Quattro, J. M. (1992). Analysis of molecular variance inferred from metric distances among DNA haplotypes: Application to human mitochondrial DNA restriction data. *Genetics*, *131*, 479–491.

Ferretti, F., Myers, R. A., Serena, F., & Lotze, H. K. (2008). Loss of large predatory sharks from the Mediterranean Sea. *Conservation Biology*, *22*, 952–964.

Foster, S. D. (2020). *stockR: Identifying stocks inGenetic data*. R package version, 1.0.74.

Foster, S. D., Feutry, P., Grewe, P., & Davies, C. (2021). Sample size requirements for genetic studies on yellowfin tuna. *PLoS One*, *16*(11), e0259113.

Foster, S. D., Feutry, P., Grewe, P. M., Berry, O., Hui, F. K. C., & Campbell, R. D. (2018). Reliably discriminating stock structure with genetic markers: Mixture models with robust and fast computation. *Molecular Ecology Resources*, *18*, 1310–1325.

Fraisse, C., Roux, C., Gagnaire, P. A., Romiguier, J., Faivre, N., Welch, J. J., & Bierne, N. (2018). The divergence history of European blue mussel species reconstructed from approximate Bayesian computation: The effects of sequencing techniques and sampling strategies. *PeerJ*, *6*, e5198.

Fujinami, Y., Semba, Y., Okamoto, H., Ohshimo, S., & Tanaka, S. (2017). Reproductive biology of the blue shark (*Prionace glauca*) in the western North Pacific Ocean. *Marine and Freshwater Research*, *68*, 2018–2027.

Galván-Magaña, F., Castillo-Geniz, J. L., Hoyos-Padilla, M., Ketchum, J., Klimley, A. P., Ramírez-Amaro, S., Torres-Rojas, Y. E., & Tovar-Ávila, J. (2019). Shark ecology, the role of the apex predator and current conservation status. *Advances in Marine Biology*, *83*, 61–114. https://doi.org/10.1016/bs.amb.2019.08.005

Georges, A., Gruber, B., Pauly, G. B., White, D., Adams, M., Young, M. J., Kilian, A., Zhang, X., Shaffer, H. B., & Unmack, P. J. (2018). Genome wide SNP markers breathe new life into phylogeography and species delimitation for the problematic short-necked turtles (Chelidae: *Emydura*) of eastern Australia. *Molecular Ecology*, *27*, 5195–5213.

Gosselin, T. (2018). *Radiator: RADseq data exploration, manipulation and visualization using R*. In. R package version 0.0.11. Retrieved from https://github.com/thierrygosselin/radiator

Gosselin, T., Lamothe, M., Devloo-Delva, F., & Grewe, P. (2020). radiator: RADseq Data Exploration, Manipulation and Visualization using R. https://thierrygosselin.github.io/radiator/

Green, M. E., Appleyard, S. A., White, W., Tracey, S., Devloo-Delva, F., & Ovenden, J. R. (2019). Novel multimarker comparisons address the genetic population structure of silvertip sharks (*Carcharhinus albimarginatus*). *Marine and Freshwater Research*, *70*, 1007. https://doi.org/10.1071/mf18296

Greig, T. W., Alvarado Bremer, J. R., & Ely, B. (1999). Preliminary results from genetic analyses of nuclear markers in swordfish, Xiphias gladius, reveal concordance with mitochondrial DNA analyses. *International Commission for the Conservation of Atlantic Tunas Collective Volume of Scientific Papers*, *49*(1), 476–482.

Grewe, P., Grueger, C., Aquadro, C. F., & Berminghmam, E. (1993). Mitochondrial DNA variation among Lake trout (*Salvelinus namaycush*) strains stocked into Lake Ontario. *Canadian Journal of Fisheries and Aquatic Sciences*, *50*, 2397–2403.

Grewe, P. M., Feutry, P., Hill, P. L., Gunasekera, R. M., Schaefer, K. M., Itano, D. G., Fuller, D. W., Foster, S. D., & Davies, C. R. (2015). Evidence of discrete yellowfin tuna (*Thunnus albacares*) populations demands rethink of management for this globally important resource. *Scientific Reports*, *5*, 16916. https://doi.org/10.1038/srep16916

Gutenkunst, R. N., Hernandez, R. D., Williamson, S. H., & Bustamante, C. D. (2009). Inferring the joint demographic history of multiple populations from multidimensional SNP frequency data. *PLoS Genetics*, *5*, e1000695.

Hedgecock, D., Barber, P. H., & Edmands, S. (2007). Genetic approaches to measuring connectivity. *Oceanography*, *20*, 70–79.

Hernández-Aguilar, S. B., Escobar-Sánchez, O., Galván-Magaña, F., & Abitia-Cárdenas, L. A. (2015). Trophic ecology of the blue shark (*Prionace glauca*) based on stable isotopes (δ13C and δ15N) and stomach content. *Journal of the Marine Biological Association of the United Kingdom*, *96*(7), 1403–1410.

Hughes, B. B., Eby, R., Van Dyke, E., Tinker, M. T., Marks, C. I., Johnson, K. S., & Wasson, K. (2013). Recovery of a top predator mediates negative eutrophic effects on seagrass. *Proceedings of the National Academy of Sciences*, *110*(38), 15313–15318.

ICCAT, International Commission for the Conservation of Atlantic Tunas. (2015). *Report of the 2015 ICCAT Blue shark stock assessment session*. Retrieved from www.iccat.int. retrieved from www.iccat.in on November 28, 2022. https://www.iccat.int/Documents/CVSP/CV072_2016/n_4/CV072040866.pdf

ICCAT, International Commission for the Conservation of Atlantic Tunas. (2019). *Management Measures for the Conservation of the north Atlantic Blue Shark caught in association with ICCAT fisheries*. In, edited by retrieved from www.iccat.in on November 28, 2022. https://www.iccat.int/Documents/Recs/compendiopdf-e/2019-07-e.pdf

IOTC, Indian Ocean Tuna Commission. (2007). *Compilation of information on blue shark (Prionace glauca), silky shark (Carcharhinus falciformis), oceanic whitetip shark (Carcharhinus longimanus), scalloped hammerhead (Sphyrna lewini) and shortfin mako (Isurus oxyrinchus) in the Indian Ocean*. A working paper ed. GTEPA.

IOTC, Indian Ocean Tuna Commission. (2017). Stock assessment blue shark (*Prionace glauca*) in the Indian Ocean using Stock Synthesis. In, edited by Working Party on Ecosystems and Bycatch (WPEB).

ISC, International Scientific Committee for Tuna and Tuna-like Species in the north Pacific Ocean. (2018). Stock assessment and future projections of Blue Shark in the North Pacific Ocean through 2015. SC14-SA-IP-13. https://meetings.wcpfc.int/node/10722

Jombart, T. (2008). Adegenet: A R package for the multivariate analysis of genetic markers. *Bioinformatics*, *21*, 1403–1405.

Jombart, T., & Ahmed, I. (2011). *Adegenet* 1.3-1: New tools for the analysis of genome-wide SNP data. *Bioinformatics*, *27*, 3070–3071.

Jombart, T., Devillard, S., & Balloux, F. (2010). Discriminant analysis of principal components: A new method for the analysis of genetically structured populations. *BMC Genetics*, *11*, 94.

Jouganous, J., Long, W., Ragsdale, A. P., & Gravel, S. (2017). Inferring the joint demographic history of multiple populations: Beyond the diffusion approximation. *Genetics*, *206*(3), 1549–1567.

Kaiser, J., Schefuß, E., Lamy, F., Mohtadi, M., & Hebbeln, D. (2008). Glacial to Holocene changes in sea surface temperature and coastal vegetation in north Central Chile: High versus low latitude forcing. *Quaternary Science Reviews*, *27*, 2064–2075.

Kamm, J., Terhorst, J., Durbin, R., & Song, Y. S. (2020). Efficiently inferring the demographic history of many populations with allele count data. *Journal of the American Statistical Association*, *115*(531), 1472–1487.

Kamvar, Z. N., Tabima, J. F., & Grünwald, N. J. (2014). Poppr: An R package for genetic analysis of populations with clonal, partially clonal, and/or sexual reproduction. *PeerJ*, *2*, e281–e281.

Keenan, K., McGinnity, P., Cross, T. F., Crozier, W. W., & Prodöhl, P. A. (2013). diveRsity: An R package for the estimation and exploration of population genetics parameters and their associated errors. *Methods in Ecology and Evolution*, *4*, 782–788.

Kilian, A., Wenzl, P., Huttner, E., Carling, J., Xia, L., Blois, H., Caig, V., Katarzyma, H.-U., Jaccoud, D., Hopper, C., Aschenbrenner-Kilian, M., Evers, M., Peng, K., Cayla, C., Hok, P., & Uszynski, G. (2012). Diversity arrays technology: A generic genome profiling technology on open platforms. *Methods in Molecular Biology (Methods and Protocols)*, *888*, 67–88.

King, J. R., Wetklo, M., Supernault, J., Taguchi, M., Yokawa, K., Sosa-Nishizaki, O., & Withler, R. E. (2015). Genetic analysis of stock structure of blue shark (*Prionace glauca*) in the North Pacific Ocean. *Fisheries Research*, *172*, 181–189.

Kohler, N. E., & Turner, P. A. (2008). *Stock structure of the blue shark (Prionace glauca) in the North Atlantic Ocean based on tagging data* (pp. 339–350). Sharks of the Open Ocean: Biology, Fisheries and Conservation.

Kohler, N. E., Turner, P. A., Hoey, J. J., Natanson, L. J., & Briggs, R. (2002). Tag and recapture data for three pelagic shark species: Blue shark (*Prionace glauca*), shortfin Mako (*Isurus oxyrinchus*), and porbeagle (*Lamna nasus*) in the North Atlantic Ocean. *Collective Volume of Scientific Papers*, *54*, 1231–1260.

Leduc, G., Schneider, R., Kim, J. H., & Lohmann, G. (2010). Holocene and Eemian Sea surface temperature trends as revealed by alkenone and Mg/Ca paleothermometry. *Quaternary Science Reviews*, *29*, 989–1004.

Leone, A., Urso, I., Damalas, D., Martinsohn, J., Zanzi, A., Mariani, S., Sperone, E., Micarelli, P., Garibaldi, F., Megalofonou, P., Bargelloni, L., Franch, R., Macias, D., Prodohl, P., Fitzpatrick, S., Stagioni, M., Tinti, F., & Cariani, A. (2017). Genetic differentiation and phylogeography of Mediterranean-north eastern Atlantic blue shark (*Prionace glauca*, L. 1758) using mitochondrial DNA: Panmixia or complex stock structure? *Peerj*, *5*, 18.

Leslie, M. S., & Morin, P. A. (2016). Using genome-wide SNPs to detect structure in high-diversity and low-divergence populations of severely impacted eastern tropical Pacific spinner (Stenella longirostris) and pantropical spotted dolphins (*S. attenuata*). *Frontiers in Marine Science*, *3*, 253. https://doi.org/10.3389/fmars.2016.00253

Li, W. W., Dai, X. J., Zhu, J. F., Tian, S. Q., He, S., & Wu, F. (2017). Genetic differentiation in blue shark, *Prionace glauca*, from the Central Pacific Ocean, as inferred by mitochondrial cytochrome b region. *Mitochondrial DNA Part A*, *28*, 575–578.

Luu, K., Bazin, E., & Blum, M. G. B. (2017). Pcadapt: An R package to perform genome scans for selection based on principal component analysis. *Molecular Ecology Resources*, *17*, 67–77.

Mamoozadeh, N. R., Graves, J. E., & McDowell, J. R. (2020). Genome-wide SNPs resolve spatiotemporal patterns of connectivity within striped marlin (*Kajikia audax*), a broadly distributed and highly migratory pelagic species. *Evolutionary Applications*, *13*, 677–698. https://doi.org/10.1111/eva.12892

Masson-Delmotte, V., Schulz, M., Abe-Ouchi, A., Beer, J., Ganopolski, A., González Rouco, J. F., Jansen, E., Lambeck, K., Luterbacher, J.,

Naish, T., Osborn, T., Otto-Bliesner, B., Quinn, T., Ramesh, R., Rojas, M., Shao, X., & Timmermann, A. (2013). Information from paleo-climate archives. In T. F. Stocker, D. Qin, G.-K. Plattner, M. Tignor, S. K. Allen, J. Boschung, A. Nauels, Y. Xia, V. Bex, & P. M. Midgley (Eds.), *Climate change 2013: The physical science basis. Contribution of working group I to the fifth assessment report of the intergovernmental panel on climate change.* Cambridge University Press.

Matsunaga, H., & Nakano, H. (1999). Species composition and CPUE of pelagic sharks caught by Japanese longline research and training vessels in the Pacific Ocean. *Fisheries Science, 65*, 16–22.

Maxwell, S. M., Scales, K. L., Bograd, S. J., Briscoe, D. K., Dewar, H., Hazen, E. L., Lewison, R. L., Welch, H., & Crowder, L. B. (2019). Seasonal spatial segregation in blue sharks (*Prionace glauca*) by sex and size class in the Northeast Pacific Ocean. *Diversity and Distributions, 25*, 1304–1317.

Megalofonou, P., Dimitris, D., & de Metrio, G. (2005). Size, age and sexual maturity of the blue shark, *Prionace glauca*, in the Mediterranean Sea. *Biology*, CM 2005/N:09.

Megalofonou, P., Yannopoulos, C., Damalas, D., de Metrio, G., Deflorio, M., & de la Serna, J. M. (2005). Incidental catch and estimated discards of pelagic sharks from the swordfish and tuna fisheries in the Mediterranean Sea. *Fishery Bulletin, 103*, 620–634.

Mejuto, J., & Garcia-Cortés, B. (2005). Reproductive and distribution parameters of the blue shark *Prionace glauca*, on the basis of on-board observations at sea in the Atlantic, Indian and Pacific oceans. *Collective Volume of Scientific Papers ICCAT, 58*(3), 951–973.

Momigliano, P., Harcourt, R., Robbins, W. D., Jaiteh, V., Mahardika, G. N., Sembiring, A., & Stow, A. (2017). Genetic structure and signatures of selection in grey reef sharks (*Carcharhinus amblyrhynchos*). *Heredity (Edinb), 119*, 142–153.

Mullins, R. B., McKeown, N. J., Sauer, W. H. H., & Shaw, P. W. (2018). Genomic analysis reveals multiple mismatches between biological and management units in yellowfin tuna (*Thunnus albacares*). *ICES Journal of Marine Science, 75*, 2145–2152.

Murua, H., Eveson, J. P., & Marsac, F. (2015). The Indian Ocean tuna tagging programme: Building better science for more sustainability preface. *Fisheries Research, 163*, 1–6.

Nakano, H., & Clarke, S. (2005). Standardized CPUE for blue sharks caught by the Japanese longline fishery in the Atlantic Ocean, 1971–2003. *ICCAT Collective Volume of Scientific Papers, 58*, 1127–1134.

Nakano, H., & Seki, M. P. (2003). Synopsis of biological data on the blue shark, *Prionace glauca* Linnaeus. *Bulletin-Fisheries Research Agency Japan, 6*, 18–55.

Nakano, H., & Stevens, J. D. (2008). The biology and ecology of the blue shark, *Prionace Glauca*. In *Sharks of the Open Ocean*. Blackwell Publishing Ltd.

Nikolic, N., Devloo-Delva, F., Bailleul, B., Noskova, E., Rougeux, C., Liautard-Haag, C., Hassan, M., Marie, A., Borsa, P., Feutry, P., Grewe, P., Davies, C., Farley, J., Fernando, D., Biton Porsmoguer, S., Poisson, F., Parker, D., Aulich, J., Lansdell, M., ... Arnaud-Haond, S. (2020). *Genome scans discriminate independent populations of the blue shark Prionace glauca. IOTC-2020-WPEB16-14.*

Nikolic, N., Montes, I., Lalire, M., Puech, A., Bodin, N., Arnaud-Haond, S., Kerwath, S., Corse, E., Gaspar, P., Hollanda, S., Bourjea, J., West, W., & Bonhommeau, S. (2020). Connectivity and population structure of albacore tuna across Southeast Atlantic and southwest Indian oceans inferred from multidisciplinary methodology. *Scientific Reports, 10*, 15657.

Noskova, E., Ulyantsev, V., Koepfli, K. P., O'Brien, S. J., & Dobrynin, P. (2020). GADMA: Genetic algorithm for inferring demographic history of multiple populations from allele frequency spectrum data. *GigaScience, 9*(3), giaa005.

Olsen, J., Anderson, N. J., & Knudsen, M. F. (2012). Variability of the North Atlantic oscillation over the past 5,200 years. *Nature Geoscience, 5*, 808–812.

Ovenden, J. R., Kashiwagi, T., Broderick, D., Giles, J., & Salini, J. (2009). The extent of population genetic subdivision differs among four co-distributed shark species in the Indo-Australian archipelago. *BMC Evolutionary Biology, 9*, 40.

Panayiotou, N., Biton-Porsmoguer, S., Moutopoulos, D. K., & Lloret, J. (2020). Offshore recreational fisheries of large vulnerable sharks and teleost fish in the Mediterranean Sea: First information on species caught. *Mediterranean Marine Science, 21*(1), 222–227. https://doi.org/10.12681/mms.21938

Paradis, E. (2010). Pegas: An R package for population genetics with an integrated–modular approach. *Bioinformatics, 26*, 419–420.

Pazmiño, D. A., Maes, G. E., Simpfendorfer, C. A., & van Herwerden, L. (2017). Genome-wide SNPs reveal small scale conservation units in the highly vagile Galápagos shark (*Carcharhinus galapagensis*). *Conservation Genetics, 18*, 1151–1163.

Pecoraro, C., Babbucci, M., Franch, R., Rico, C., Papetti, C., Chassot, E. I., Bodin, N., Cariani, A., Bargelloni, L., & Fausto, T. (2018). The population genomics of yellowfin tuna (*Thunnus albacares*) at global geographic scale challenges current stock delineation. *Scientific Reports, 8*, 13890.

Pembleton, L., Cogan, N., & Forster, J. (2013). StAMPP: An R package for calculation of genetic differentiation and structure of mixed-ploidy level populations. *Molecular Ecology Resources, 13*, 946–952. https://doi.org/10.1111/1755-0998.12129

Pirog, A. (2018). *Structure génétique des populations et biologie de la reproduction chez le requin bouledogue Carcharhinus leucas et le requin tigre Galeocerdo cuvier.* Ecologie, Environnement. Université de la Réunion. Français. PhD. ⟨NNT: 2018LARE0008⟩. ⟨tel-01879924⟩.

Porcher, L. E., & Darvell, B. W. (2022). Shark fishing vs. conservation: Analysis and synthesis. *Sustainability, 14*, 9548.

Portnoy DS, McDowelll JR, Heist EJ, Musick JA, Graves JE. 2010. World phyl,- ogeography and male-mediated gene flow in the sandbar shark, *Carcharhinus plumbeus. Molecular Ecology, 19*, 1994–2010.

Queiroz, N., Humphries, N. E., Noble, L. R., Santos, A. M., & Sims, D. W. (2012). Spatial dynamics and expanded vertical niche of blue sharks in oceanographic fonts reveal habitat targets for conservation. *Plos One, 7*(2), e32374.

Rigby, C. L., Barreto, R., Carlson, J., Fernando, D., Fordham, S., Francis, M. P., Herman, K., Jabado, R. W., Liu, K. M., Marshall, A., Pacoureau, N., Romanov, E., Sherley, R. B., & Winker, H. (2019). *Prionace glauca. The IUCN red list of threatened species, 2019: E.T39381A2915850.* https://doi.org/10.2305/IUCN.UK.2019-3.RLTS.T39381A2915850.en. Downloaded on 31 March 2021

Rodríguez-Ezpeleta, N., Bradbury, I. R., Mendibil, I., Álvarez, P., Cotano, U., & Irigoien, X. (2016). Population structure of Atlantic mackerel inferred from RAD-seq-derived SNP markers: Effects of sequence clustering parameters and hierarchical SNP selection. *Molecular Ecology Resources, 16*, 991–1001.

Rougeux, C., Bernatchez, L., & Gagnaire, P. A. (2017). Modeling the multiple facets of speciation-with-gene-flow toward inferring the divergence history of Lake whitefish species pairs (*Coregonus clupeaformis*). *Genome Biology and Evolution, 9*, 2057–2074.

Sansaloni, C., Petroli, C., Jaccoud, D., Carling, J., Detering, F., Grattapaglia, D., & Kilian, A. (2011). Diversity arrays technology (DArT) and next-generation sequencing combined: Genome-wide, high throughput, highly informative genotyping for molecular breeding of eucalyptus. *BMC Proceedings, 5*, 54.

Shevenell, A. E., Ingalls, A. E., Domack, E. W., & Kelly, C. (2011). Holocene Southern Ocean surface temperature variability west of the Antarctic peninsula. *Nature, 470*, 250–254.

Simpfendorfer, C. A., Hueter, R. E., Bergman, U., & Connett, S. M. H. (2002). Results of a fishery-independent survey for pelagic sharks in the western North Atlantic, 1977-1994. *Fisheries Research, 55*, 175–192.

Sims, D., Fowler, F. L., Ferretti, F., & Stevens, J. (2016). *Prionace glauca. The IUCN Red List of Threatened Species, 2016: e.T39381A16553182*.

Sovic, M., Fries, A., Martin, S. A., & Lisle, H. G. (2019). Genetic signatures of small effective population sizes and demographic declines in an endangered rattlesnake, *Sistrurus catenatus*. *Evolutionary Applications, 12*, 664–678.

Stevens, J. (2009). *Prionace glauca. The IUCN Red List of Threatened Species, 2009: e.T39381A10222811*. http://web.archive.org/web/20180412085123/http://www.iucnredlist.org/details/39381/0. Downloaded on 12 April 2021.

Stevens, J. D. (1990). Further results from a tagging study of pelagic sharks in the north-East Atlantic. *Journal of the Marine Biological Association of the United Kingdom, 70*, 707–720.

Taguchi, M., King, J. R., Wetklo, M., Withler, R. E., & Yokawa, K. (2015). Population genetic structure and demographic history of Pacific blue sharks (*Prionace glauca*) inferred from mitochondrial DNA analysis. *Marine and Freshwater Research, 66*, 267–275.

Vandeperre, F., Aires-da-Silva, A., Fontes, J., Santos, M., Santos, R. S., & Afonso, P. (2014). Movements of blue sharks (*Prionace glauca*) across their life history. *PLoS One, 9*, 14.

Verissimo, A., Sampaio, I., McDowell, J. R., Alexandrino, P., Mucientes, G., Queiroz, N., da Silva, C., Jones, C. S., & Noble, L. R. (2017). World without borders: Genetic population structure of a highly migratory marine predator, the blue shark (*Prionace glauca*). *Ecology and Evolution, 7*, 4768–4781.

Waples, R. S. (1998). Separating the wheat from the chaff: Patterns of genetic differentiation in high gene flow species. *Journal of Heredity, 89*, 438–450.

Waples, R. S., & Gaggiotti, O. E. (2006). What is a population? An empirical evaluation of some genetic methods for identifying the number of gene pools and their degree of connectivity. *Molecular Ecology, 15*, 1419–1439.

Waples, R. S., Punt, A. E., & Cope, J. M. (2008). Integrating genetic data into management of marine resources: How can we do it better? *Fish and Fisheries, 9*, 423–449.

West, G., Stevens, J., & Basson, M. (2004). *Assessment of blue shark population status in the Western South Pacific. AFMA projectR01/1157* (p. 139). CSIRO Marine Research.

Whitlock, M. C., Lotterhos, K. E., & Bronstein, L. (2015). Reliable detection of loci responsible for local adaptation: Inference of a null model through trimming the distribution of FST. *The American Naturalist, 186*, S24–S36.

SUPPORTING INFORMATION

Additional supporting information can be found online in the Supporting Information section at the end of this article.